Idaho Department of Water Resources

Open File Report

FLUORESCENT DYE TRACER TEST
from the
STRICKLAND WELL
with
Quaternary/Tertiary Geologic Controls

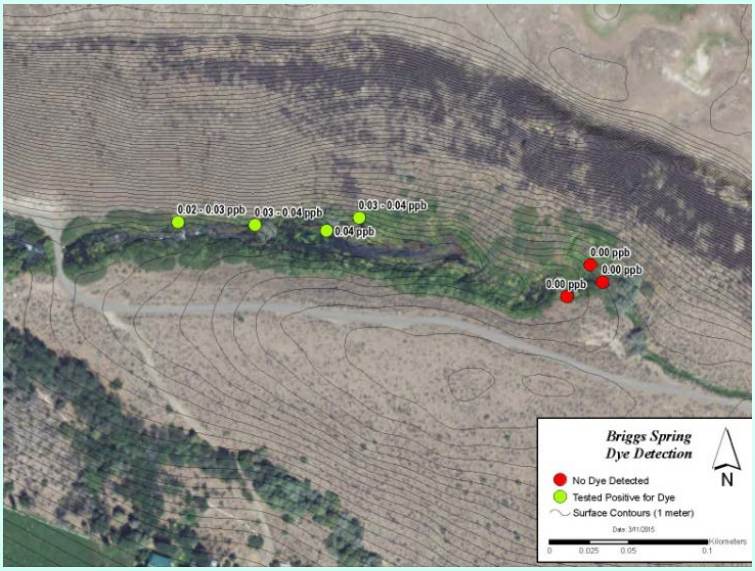

By
Neal Farmer - Idaho Department of Water Resources

And
David Blew - Idaho Power

October 19, 2022

ABSTRACT

Conducting groundwater dye tracer tests have proven to be an effective and efficient method for obtaining essential data to characterize the East Snake Plain Aquifer. A dye trace was conducted from a well (Strickland) located in Gooding County, Idaho, at Township 8 South, Range 14 East, Section 36AAA. The injection was video recorded on November 14, 2013 inside the well and the dye flowed west approximately 3.5 miles to Banbury and Briggs Springs. There have been no known previous traces performed to these springs. Results of the trace showed a westward flow path, along a 'plateau' or 'flat' low gradient groundwater table. The groundwater surface was generated from a high-resolution measurement and mapping exercise conducted in year 2013. The 'flat' water table where this trace flowed is opposite of all previous traces completed prior to 2013. The previous traces in the Malad Gorge area flowed down steeper trough shaped features in the water table. This report also presents an evaluation of geologic information related to low permeable subsurface geologic feature that appears to split the dye cloud near the spring area.

TABLE OF CONTENTS

Abstract 1
Background 4
Study Area 4
Methods and Materials 6
Results 8
  Breakthrough Curves 10
  Briggs Spring 11
  Banbury Spring 12
  Blind Canyon and Box Canyon Springs 12
Discussion Geologic Controls 13
  Blind Canyon Spring 14
  Banbury Spring 14
  Briggs Spring 15
  3-D Quaternary Tertiary Geologic Contact Model 16
Dye Flow Path Discussion 18
Groundwater Velocity 19
Reynolds and Peclet Numbers 20
Conclusions 22

LIST OF ILLUSTRATIONS

Figure 1 Location of Strickland Trace 23
Figure 2 Cavernous Basalt Well Video Image 24
Figure 3 Groundwater Gradient Map 25
Figure 4 Monitoring Locations for Strickland Trace 26
Figure 5 Early Groundwater Velocity Chart 27
Figure 6 Initial Wells Testing Postive 28
Figure 7 Wells Sampled for Lab Analsyis 29
Figure 8 Breakthrough Curves for Wells and Springs 31
Figure 9 Briggs Spring Field Sample Sites 32
Figure 10 Dye Breakthrough Curve from Briggs and Banbury Spring 33
Figure 11 Outcrop of Glenns Ferry Formation at Blind Canyon 36
Figure 12 Image of Banbury Spring from Covington and Weaver 1991 37
Figure 13 Total Area of 3-D Model of the QT Contact 38
Figure 14 3-D QT Contact Model of Strickland Trace Area 39
Figure 15 Water Table Map 40
Figure 16 Isochore Map of Trace Area 41
Figure 17 Specific Conductivity Flow Zones 42
Figure 18 Isopeths of Specific Conductance 43
Figure 19 Dye Trace Relation between Dominant Velocity and Gradient 44
Figure 20 Dye Trace Relation between Dominant Velocity and Distance 45
Figure 21 Reynolds Numbers Based on Dye Tracing 46
Figure 22 Peclet Numbers for Strickland Trace 47

Table 1 Comparison of Interpolated Transverse Dispersion 29
Table 2 Results of Lab Analysis from Water Samples at Wells 30
Table 3 Results of Lab Analysis from Water Samples at Briggs Spring 32

Table 4 Results of Lab Analysis from Charcoal Packets at Briggs Spring 32
Table 5 Results of Lab Analysis from Water Samples at Banbury Spring 34
Table 6 Groundwater Velocities from the Strickland Well to Briggs and Banbury Spring 34
Table 7 Results of Charcoal Packet Analysis at Banbury Springs 34
Table 8 Results of Lab Analysis from Water Samples at Blind and Box Canyon Areas 35
Table 9 Results of Lab Analysis from Charcoal Samples at Blind and Box Canyon Areas 35

References 48

BACKGROUND

The 'Strickland' well trace is the nineteenth trace successfully completed in a series of traces through a cooperative effort between the Idaho Department of Water Resources (IDWR), Idaho Power Company (IPC), landowners and other entities (Farmer & Blew, 2009, 2010, 2011, 2012, 2014a; Farmer, Blew, & Aley, 2014b). Previous tracer studies in this series have followed an iterative process where each subsequent new trace builds on information from preceding traces. Locations of new traces are based on previous tracer results, groundwater table maps and other available data. The Strickland trace was the second trace location conducted in the Clear Lakes area, but the only trace conducted from this well. It followed the Ashmead Traces (Farmer & Blew, 2014a) completed in 2012 and 2013. The Strickland well was selected based on the results of the Ashmead trace projected upgradient to this general area and detailed high-resolution groundwater contour maps, a cooperative homeowner, a well with new design standards, and a well drilling report.

Study Area

The Clear Lakes spring complex spans approximately 1.2 miles along the Snake River providing water for several large trout farms and discharging water in excess of 450 cubic feet per second. Large spring complexes located downstream or westward of the Clear Lakes area include Briggs Spring, Banbury Springs, Blind Canyon Springs and Box Canyon Springs (Figure 1). Some springs discharge from the aquifer through talus slopes producing a distributed pattern but other springs can be from well-defined outlets causing a more 'point' discharge character.

Briggs Spring is located west of Clear Lakes approximately 1 mile and discharged approximately 95 cfs during the trace (USGS Gage 13095175). This spring consists of a main large discharge area with numerous smaller springs and seeps located downstream. The highest visible spring discharge was GPS'd at an elevation of 3042 ft. Other smaller seeps are obvious, but the complex appears to be generally limited to approximately 900 feet extending downstream from the main point of emergence. The head spring and seeps form a stream that discharge to the Snake River. A road crosses the stream at the USGS Gage and all of the water in the stream passes through a culvert under the road. The main dye sampling location is at the USGS Gage which is on the northside of the channel. Samples for laboratory analysis were also collected at the head spring and a diversion located approximately 450 feet down stream of the USGS gage.

Banbury Springs is located approximately 3 miles west of Clear Lakes Springs with a discharge ranging from 70 to 100 cfs. Banbury Springs discharges along a geologic contact between the overlying Flat Top Butte Basalt and the underlying Tertiary rocks. This contact exhibits a linear feature apparently dipping from north to south based on field observations. The horizontal feature is approximately 2,200 feet long and sets high on the canyon wall with the main discharge zone ranging from a low band of springs located approximately 3,050 feet and a higher level at about 3,090 feet (Figure 12). A small collection ditch carries a large volume of water to the south that cascades down a rocky slope into Morgan Lake, or it is diverted into a pipeline and carried across the Snake River. Generally, spring discharge is lower on the north side than the south side evident by the number of springs visible and the flows into Morgan

Lake. Monitoring occurred in the small collection ditch at the southern end of the complex called Banbury South. Monitoring at the northern edge of the complex occurred in the small stream above Morgan Lake called Banbury North. All discharge from Banbury Springs flows into Morgan Lake before entering the Snake River. Total discharge from the spring complex is 75 to 85 cfs according to unpublished flow rates from Idaho Power. Occasional sampling also occurred at the point where Morgan Lake discharges into the Snake River.

A smaller spring (aka Banbury Road Spring) approximately 1,500 feet north of the Banbury Springs complex was also sampled (Figure 4). The spring discharge appears to be confined to a small area at an elevation of approximately 3112 feet. This spring discharge point is approximately 20 feet higher than the Banbury Springs south side. Total discharge is estimated to be between 3 to 5 cfs. Flow in the spring enters a steep channel that flows into the Snake River approximately 1100 feet downgradient from the head of the spring.

Blind Canyon Springs are located approximately 4 miles from the Clear Lakes area and discharge approximately 12 cfs. Box Canyon Springs is located approximately 4.3 miles downstream along the Snake River from Clear Lakes Springs. The main discharge of 300 cfs emerges from a single point at the headwall alcove with numerous dispersed springs flowing into the canyon downstream dominantly from the southside of the canyon.

The general geology of the area is dominated by highly conductive Quaternary grey colored basalts deposited onto Tertiary rock types consisting of both clay rich flood plain lake sediments (Glenns Ferry Formation - GFF) and underlying low conductive brown colored basalt flows (Whitehead, 1992). The Q/T contact is extensively eroded into an undulatory geometry and is a major control for spring discharge characteristics (Malde, 1971 & 1991). Springs flow from where the Q/T contact is below the water table and the large discharge springs are associated with canyon filling lavas and pillow related rock features (Lindholm, 1993).

The Strickland trace was preceded by three tracer tests conducted from the Ashmead well, which is located approximately 2,170 feet north of Clear Springs (Figure 3). The dominant velocity (based on the peak of the breakthrough curve) for the three Ashmead tracer tests were approximately 1,630 ft/day and maximum velocities were approximately 3,000 ft/day. The transverse dispersivity, at the Clear Springs was measured at 600 feet wide.

The Strickland well lies approximately 7,000 feet northeast of the Ashmead well and was assumed to be upgradient along the same flow path line. The Strickland well (IDWR well #430215) is a 6-inch domestic well completed in April 2011 to a depth of 123 feet. The surface seal extends to 39 feet below land surface and the borehole is uncased below the surface seal. According to the well log, the underlying geology recorded was mostly fractured with some sections of competent basalts. A video log of the well prior to dye injection reveals basalt rubble zones, caverns, bulbous features that may be pillow lavas, and massive sections of basalt (Figure 2). The video log also shows a strong downhole flow and resultant gradient that starts just below the water table, approximately 62 feet below ground surface, with increased flow

rate at about 80 feet below ground surface. Video recording during the dye injection confirm the high downhole gradient. Based on high-resolution water table contours produced by Farmer and Blew (2014b) and using a particle tracking analysis (ESRI, 3D Analyst Tools, Create Steepest Path) the dye emergence area from the Strickland well was estimated to be 1,150 feet west of where dye emerged from the Ashmead traces. The trace was predicted to follow a curvilinear path approximately 11,000 feet in length from the well to the west side of Clear Springs discharge area (Figure 3).

Methods and Materials

Prior to the tracer test, water samples were collected from the target springs and sent to Ozark Underground Laboratory (OUL) for analysis. All samples tested negative for the presence of sodium fluorescein. Monitoring for dye during the trace was accomplished using charcoal packets, submersible fluorometers, and 50 mL grab water samples. Charcoal packets adsorb and concentrate dye and serve as sentinels for detecting dye (Tom Aley, 2002). Charcoal packets were placed at six spring locations and toilet reservoirs of nine homes along the projected dye flow path. Grab samples and charcoal packets were sent to OUL for analysis. During the trace, monitoring locations were adjusted as needed to meet the actual flow path of the injected dye. Positive detections of dye are based on either detection by a submersible fluorometer along with charcoal packets or grab water samples analyzed at OUL. Dye concentration trends obtained from in-situ instruments, or a series of grab samples, provide additional evidence for presence of sodium fluorescein. Submersible C3 fluorometers were installed in four spring locations. The C3 instrument is a field fluorometer produced by 'Turner Designs' that can be calibrated and programmed to deploy insitu and left to record data or used as a mobile roving instrument to test waters for fluorescein dye.

Field fluorometer data from the trace differ from laboratory analyses of samples and is due to differences in field and lab techniques and conditions. Samples analyzed by OUL are pH adjusted and filtered and the analysis is completed with a scanning spectrofluorophotometer (Thomas Aley & Beeman, 2015). This methodology allows for the detection of dye at much lower levels and more accurately than field fluorometers and concentration of dye in this study are generally less than 0.10 ppb. The minimum detection limit for the C3 field fluorometer is 0.01 ppb for FL. Debris in the in-situ spring water can cause interference noise in field data but the lab filters out sediment from samples. Laboratory analysis of grab water samples and charcoal packets were used to validate the presence of dye and support the field fluorometer data.

The initial monitoring plan included 11 wells and six spring locations shown in Figure 4 with yellow circle symbols. Sites were selected based on accessibility and position to the expected dye flow path. Three of those wells included the injection well and two nearby wells that were sampled 24 hours post injection and were negative for dye. Results of the OUL laboratory analysis can be found in Table 2. Laboratory analysis of water samples from wells was performed to provide confirmation of field fluorometer data for some sites.

Monitoring for dye commenced the day after the injection and occurred at three locations adjacent to the injection well. Water samples were collected from the injection well and tested for bacteria. Seven days post injection, on November 21, 2013, a submersible fluorometer was used to assess the presence of dye at all monitoring locations. On November 24, 2013, (10 days post dye release) the study area was expanded and additional monitoring sites were added shown in Figure 4 with blue, green and red circle symbols. At the completion of the study there were 29 wells and 17 spring locations that were monitored for the presence of dye. Monitoring for dye continued through March of 2014 (4 months post release) at which time no dye was detectable at any sample locations.

A late fall injection was planned to eliminate the influence of pumping at irrigation wells and leakage from irrigation canals and laterals. Prior to the injection a video log was completed in the well to evaluate the subsurface conditions. Video showed a strong downhole flow started about 80 feet below top of casing (BTOC). The dye injection started at 3:08 pm MST on November 14, 2013. Water level in the well was 62.32 feet BTOC. A solution of 6 gallons of water and 6 pounds of a 75% concentration of sodium fluorescein were mixed in a 15-gallon plastic tank. A small diaphragm pump attached to the tank was used to pump the dye solution from the mixing tank into the well. Weighted polyethylene tubing was attached to the mixing tank and lowered to a point near the bottom of the borehole at 105 feet depth or approximately 20 feet above the bottom of the well. A downhole camera was lowered into the well to insure proper positioning of the injection tubing. The camera was used during the injection to video record the dye release. The polyethylene tubing was purged of air prior to the release of the dye mixture.

Dye injection occurred for approximately six minutes followed by five minutes of rinse water to flush remaining dye from the injection line. Downhole video showed no visible dye after 11 minutes. The video shows dye flowing downward and exiting the borehole below 105 feet BTOC. This would be approximately 43 feet below the static water level in the well. Visual evidence documents a rapid evacuation of dye from the borehole and entrance into the surrounding aquifer. A sample collected from the well approximately 24 hours post injection tested negative for dye based on OUL laboratory analysis.

Three additional wells adjacent to the Strickland injection well were tested for dye one day post-injection. These wells were less than 500 feet from the injection well and appear to be cross gradient to the injection well. No dye was present these wells. The injection well was tested for the presence of coliform bacteria which was negative.

The observed high flow and downhole gradient has been videoed in other wells near spring areas. Previous tracer tests near springs in the Malad Gorge area, Box Canyon, and Clear Springs have also documented a high downhole gradient (Farmer & Blew, 2012, 2018; Farmer et al., 2014b) up to 3 miles from the springs. The importance of this phenomenon for tracer studies is to provide evidence that no dye is retained within the borehole. The full amount of dye injected into the well reaches the surrounding aquifer and is available for detection at sampling locations downgradient of the injection well.

Results

Dye Path

GIS based modeling showed a 'steepest' flow path to the Clear Lakes spring complex at a length of approximately 11,000 feet (≈2.0 miles) shown on Figure 3. The flow velocity for this trace was estimated to be approximately 500 ft/day based on available tracer data (Figure 5). The plot in Figure 5 indicates that a logarithmic relation exists between distance from the springs and groundwater flow velocity. Greater aquifer transmissivity and lower hydraulic gradients occur to the east, which result in slower groundwater flow velocities further from spring discharge sites (Farmer, 2021).

Increased frequency of measurements began 7 days post-injection. Initial efforts concentrated on wells considered to be downgradient of the injection well but dye was not detected at these sites. Ten days post-injection additional wells and springs were checked using a 'rover' submersible fluorometer. The first dye was detected 11 days post-injection at well sample sites located one mile west of Strickland at Chavez, BCD 1, and BCD 66 (Figure 4). Well BCD 1 had a concentration of 1.27 ppb FL from a grab water sample analyzed by the OUL laboratory. The field instrument recorded a value of 0.77 ppb for BCD 1, 0.37 ppb for Chavez and 0.65 ppb for BCD 66. The wells north (BCD 2) and south (Conner 'north') of these wells had no detection of dye using field instruments.

Based on the positive tests for dye at the newly added monitoring locations, a second analysis was done to determine potential spring locations of dye emergence using GIS 'Steepest Path' tool. The GIS modeling indicated that dye would still likely resurge in the west end of the Clear Lakes spring complex (Figure 6). Dye monitoring continued at the original monitoring sites (yellow circles in Figure 4) along with additional monitoring sites farther west (Figure 4).

On December 4th, (20 days post-injection) the Mink Farm well (Figure 4) tested positive for dye at 0.094 ppb based on results from OUL. Laboratory analysis of a sample collected on December 6th showed a dye concentration of 0.076 ppb. This well is located approximately 2.25 mile west southwest of the injection well. Sampling continued at all locations even though it was suspected that the dye would not flow to the Clear Lakes Spring complex.

By the end of the trace seven wells and two spring complexes tested positive repeatedly for dye from OUL lab results. Dye was detected from lab results in a charcoal packet in Box Canyon and Blind Canyon and one additional well (Carpenter) (Figure 4). Not enough data was collected at these sites to establish trends so they are interpreted as possible dye routing locations.

Transverse dispersion can be interpolated based on the distance between wells testing negative for dye and wells testing positive for dye. On November 25, 11 days post release and at 1.1 miles west (Figure 4), the dye cloud had a transverse dispersion of not more than 2,900 feet based on zero dye detection using a C3 field instrument at BCD 2 and Conner North wells. Between BCD 2 and Conner north wells, positive C3 measurements were observed at Chavez (0.37 ppb), BCD 1 (0.77 ppb) and BCD 66 (0.65 ppb). OUL lab analyzed the sample collected at

BCD 1 which resulted in a dye concentration of 1.27 ppb. It is concluded that BCD 1 and BCD 66 also had dye based on the trend and field instrument results though they did not have lab confirmation. Using C3 data and lab data, the dye cloud width was measured at approximately 500 feet between Chavez and BCD 66. Interpolating between the north and south zero detections of the dye cloud could have been approximately 1,500 feet wide. The ratio of lateral spread at 1.1 miles is approximately 0.25, which is about half the value compared to other traces (Table 1). On December 4th and 6th, at 2 miles distance, the dye cloud had a transverse dispersion of not more than 3,200 ft (Figure 4) based on lab results of dye concentration at the Mink Farm well (0.094 ppb and 0.076 ppb) and no detection of dye to the north and south at wells BCD 4 and Van Dyke 3 using the field fluorometer. The actual transverse dispersion width is likely narrower than 3,200 feet and inferred to be in the range of 2,000 feet.

The Anderson well, located 0.75 miles west of the dye injection well, seems to be positioned on the south edge of the cloud trajectory, and multiple field fluorometer measurements resulted in no detections of dye at this site (Figure 4). No well log is available for this well and based on field observations for this type of construction, the well likely dates prior to the 1970s. It is the authors experience that wells drilled during this period may only have a few feet of water in the well. The depth of dye injection may be lower than the bottom of the borehole for the Anderson well. The dye was released 43 feet below the water table in the Strickland well with a strong downward flow and gradient potentially routing the dye to deeper depths. Therefore, it is a possibility that the Anderson well, being older and probably shallower, may be completed at a higher elevation and the dye cloud passed beneath the well; or, it is simply on the south edge of the dye cloud and not in the flow path. The Anderson well is also located between 2 canals with a possible localized gradient caused by leaky canals and diverting the dye on a more northerly route. Combined with sparse sampling using field instruments, these factors may provide possible explanations for the absence of dye at the Anderson well.

The groundwater table falls approximately 58 feet for the first 1.7 miles of the dye cloud flow path for a gradient of 0.006 (ft/ft) (Figure 6). At this point the dye cloud encounters a noticeable flattening in the water table gradient to 0.003 for approximately 6,643 feet. This change in gradient may be due to subsurface geology, which is splitting the dye cloud to Banbury Springs and Briggs Springs. The water may also flow towards Blind Canyon and Box Canyon springs. At 2.9 miles downgradient from the injection well, the dye cloud has apparently split and is flowing towards Briggs Springs and Banbury Springs. There was no detection of dye at the Montgomery Home and Montgomery Rental wells, but dye was detected both north and south of these wells suggesting a split in the dye cloud. Adjacent to Brigg Springs, the gradient increases to 0.028 for the last 2,800 feet and for Banbury the gradient increase to 0.017 for the last 2,250 feet. The trace to Briggs Springs was approximately 19,000 ft and Banbury Springs was approximately 18,750 ft. The overall groundwater gradient to Briggs Springs was 0.008 and to Banbury Springs was 0.006 and Banbury spring is at a higher elevation than Briggs spring by 50 feet.

Breakthrough Curves

Figure 8 shows partial dye concentration breakthrough curves for wells and two spring sites along the main flow path. Field measurements were made with a C3 fluorometer and the instrument data was calibrated to lab results from grab water samples collected at the same time as the field measurements. The peak of the breakthrough curve is used for calculating dominant velocity. Well BCD 1 was the first well along the flow path and it had the highest concentration at 1.27 ppb (lab) at 11 days as displayed with solid red diamond symbols. The data for this well has higher concentrations compared to the other wells so it is plotted as the only data set for the left vertical axis. The first sample may have been collected after the peak dye concentration had passed. The next well that dye flowed past was the Mink Farm well located 2.27 miles downgradient of the injection well. It tested positive for dye on 20 days post injection with a concentration of 0.094 ppb (lab); and two days later at 0.076 ppb (lab). The dark blue square symbols in Figure 8 show the calibrated breakthrough curve for this well with an apparent peak 20 days post injection on December 4th. This would result in a dominant velocity calculation of approximately 600 ft/day from the injection well to the Mink Farm well, which is consistent with the data from previous tracer studies on the East Snake Plain Aquifer (ESPA) (Figure 19). This lends confidence to the calibrated values since a high-resolution breakthrough curve was not collected at this site.

The next wells to be impacted by dye in Figure 4 are the Colona and Phillips 1 wells. A comparison of these two wells suggests that dye moved faster and at a higher concentration past the Phillips 1 well due to the higher peak concentration that occurs earlier in time than the Colona well. If the peak did occur on 29 days post injection on December 13th, then a dominant velocity would equate to approximately 508 feet/day. The apparent peak at the Colona well was 43 days post injection which would equate to approximately 348 feet/day dominant velocity. This suggests a slightly slower velocity toward Banbury Spring and a slightly higher velocity towards Briggs Spring.

As dye moved from the Colona well towards the Livia and Jones wells the peak concentration decreased slightly from 0.6 to 0.5 ppb. The Jones and Livia wells are close to each other, and water samples were measured on the same day using a C3. Only the Jones well had a grab water sample lab result that was used for both wells to calibrate the C3 data. The breakthrough curve data for both wells are parallel to each other with a similar rising limb slope angle and peak date suggesting a common response to the passing dye cloud.

The breakthrough curves for Banbury spring southside and Briggs Spring northside are shown in Figure 8. Briggs spring received a higher concentration of dye which peaked and the recession limb dips below the data for Banbury Spring. The shape of the Briggs breakthrough curve has a typical left skew with a steep rising limb and lower angle recession limb. Periodic spikes in the data are caused by interference with the sensors by particles of sediment, algae or air bubbles. The shape of the Briggs curve supports the dye arrived in higher concentrations and dissipated faster than at Banbury spring data. The Banbury spring curve shows a similar left skew shaped curve with a steep rising limb and lower angle recession limb. The Livia, Jones, Colona wells

and Banbury spring data all appear to peak at the same time. Higher resolution data would help refine the timing of these.

Briggs Springs

A charcoal packet was installed on the south side of the culvert near the USGS gage 11 days post injection and the water at this location was tested periodically with a C3 fluorometer. At 26 days (December 10, 2013), a fluorometer was installed at Briggs Springs approximately 200 feet upstream of the USGS gage along the southern side of the stream. A water sample was collected on December 10, 2013 at the USGS gage northside with a lab result of 0.018 ppb. Laboratory analysis can be found in Table 3. At 32 days (December 16, 2013), fluorometer data showed no dye for the southside of the culvert so it was moved to the north side. The results indicated a difference in dye concentrations between the north and south side of the culvert.

At 64 days field fluorometer measurements were made to determine the location of dye emergence within the spring complex (Figure 9). Concentrations on the northside of the culvert measured 0.02 ppb and those on the southside measured 0.00 ppb. In-between the culvert and the main spring head on the northside, there are numerous smaller discharge springs. Field fluorometer measurements showed the main spring discharge area had no dye and field measurements were confirmed from laboratory results (Table 3). A low discharge spring located approximately 600 feet west of the spring head, had the highest concentration of dye emergence (0.04 ppb) according to the field fluorometer. Not all sites along the spring complex were accessible for measurements but upstream (east) and downstream (west) measurements from this site show a decrease in dye concentrations.

Field fluorometer measurements at the USGS Gage on the north side of the channel provided a breakthrough curve for Briggs Springs (Figure 10). The first confirmed dye at the site was on 26 days and the peak occurred at 45 days (December 29, 2013). The interpolated first arrival was 24 days (December 8, 2013) based on the fluorometer data and OUL laboratory results from grab samples. Field fluorometer concentrations are raw data and are higher than those reported for laboratory analysis. By February 10, 2014, the fluorometer no longer recorded the presence of dye and on March 25, 2014 a lab result showed no detection of dye. The fluorometer data indicates a total time for dye passage of 88 days. The maximum velocity of 700 ft./day is based on the first arrival of dye at the point of emergence. The dominant velocity of 404 ft./day is based on the time to peak dye emergence.

Sampling at the head spring was limited but suggests the head spring was not a point of dye emergence, or it was not the site of highest dye concentration. Charcoal packet analysis shows a large difference between dye concentrations on the southern and northern sides of the Briggs Springs flow channel (Table 4). Charcoal packets were placed less than 25 feet apart on the north and south sides of the culvert near the USGS Gage (Figure 9). The packet on the southern side was placed on December 1, 2013 and the north packet was placed two weeks later on December 15, 2013. Despite the longer exposure time of the southern packet, the packet on the north side of the channel had approximately 9 times the dye concentration. Dye emergent areas appear to be limited to the springs and seeps along the northern side of the channel

limiting the mixing of dye within the channel and causing a propensity of the dye to flow along the northside of the channel.

Banbury Springs

Monitoring began in the Banbury Springs area 10 days post injection (November 11, 2013), with the placement of charcoal packets at Banbury Road Spring. On November 26, charcoal packets were placed at Banbury North and South monitoring locations. Sampling using a submersible fluorometer and grab samples for laboratory analysis began on December 6th (Table 5). The first positive hit for dye (0.040 ppb) was at 27 days (December 10, 2013), from a grab water sample collected at Banbury South. Within the Banbury complex, including the Banbury Road Spring, only Banbury South and the Morgan Lake discharge sites had water samples that tested positive for dye. The Banbury North location did test positive for dye in a charcoal packet, but no water samples tested positive at this location which is common when water concentrations are below the detection limit. The Morgan Lake discharge is a composite of all discharge from within the spring complex and dye results at this location are likely diluted.

A field fluorometer was installed at the Banbury North and South sites. The North site fluorometer did not register any positive detection of dye. Equipment at the South site experienced several problems including a failure due to human disturbance. Lab results from the South site does provide some information on a breakthrough curve. The first dye detection occurred on December 10 the same date as the first known detection at Briggs Springs (Figure 10) and the peak concentration occurred on December 27 at the same as Briggs spring. The maximum velocity was calculated at 706 ft/day and the dominant groundwater velocity was calculated at 427 ft/day to the Banbury Springs south side.

Charcoal packets were installed at Banbury North and South monitoring locations. A charcoal packet was also placed in Banbury Road Spring but was not recoverable. Results of the charcoal packet analysis can be found in Table 7. The data indicates that dye was present at both North and South sites but the response at the South was much higher. Most of the dye appears to have been concentrated along the southern edge of the Banbury Spring complex.

Blind Canyon and Box Canyon Springs

Several samples from Blind Canyon and Box Canyon Springs tested positive for dye either by charcoal packet or water sample. The source water for these areas is derived from spring sources. Lab results of water samples can be found in Table 8 and lab results of charcoal packet Table 9. The Carpenter well tested positive for dye from a water sample on December 27 but no detection of dye on January 17. The Gill well had a no detection on both December 27 and January 17 from water samples. There were not enough samples collected to confirm a trend from the dye detections in these wells but, based on the timing and ongoing monitoring, those detections could be associated with the dye trace.

Discussion

Geologic Controls

Understanding the flow paths of dye to spring locations requires an evaluation of the geologic controls of the springs. For over 100 years, USGS scientists have been studying the geologic controls of springs from the ESPA. The geologic contact between overlying Quaternary rocks and underlying Tertiary rocks is a major control on spring characteristics. Basalt is the dominant rock type of the overlying Quaternary ESPA host rock and numerous reports document the hydrogeology (Covington and Weaver, 1991; Whitehead, 1992; Lindholm, 1996). The Quaternary basalts have more fractures, pillows and associated breccia, and conduits than the denser less fractured underlying Tertiary basalts. The Tertiary rocks include both clay rich clastic Lake Idaho deposits and low permeability dense basalts described by Whitehead (1992). A sample of Tertiary Banbury basalt (580-1,075 ft below ground surface) analyzed from a test well (07S 15E 12CBA1) had vesicles filled with clay minerals and calcite (Lindholm, 1993) which reduce conductivity.

While in this Strickland trace report and in Lindholm (1993), the use of the Q/T contact is generally applied, a more accurate delineation in the greater Thousand Springs area is the contact between the Snake River Group and the Idaho Group rocks. The Q/T contact is a highly eroded unconformity and ranges in elevation from the current land surface down to depths deeper than the modern-day canyon of the Snake River (Malde, 1982). Russell (1902) identified ancient canyon filled outcrops and later in 1936 Stearns explained the process by a ‘cut’ into the Tertiary and ‘fill’ by Quaternary volcanic rocks. Malde and Powers (1971), Covington and Weaver (1985; 1991) and again Malde (1991) started mapping the profiles and subsurface extensions of these buried canyons to aid in the understanding of why springs occur at certain locations. Why are some springs are constrained tightly by dry conditions on either side of the spring and others have a more laterally continuous nature of discharge patterns? Why do discharge rates and elevations vary?

The following description of geology near spring areas for the Strickland trace is based on:

- in-situ outcrop sampling
- on-site inspection
- high vertical accuracy Trimble Geo7x cm edition GPS
- USGS topographic maps
- historical air photos
- current geologic maps
- review and ground truthing of well drilling logs
- speaking with property owners
- obtaining unique access to locations
- identification of fossils from the Glenns Ferry Formation
- review of an extensive list of historical publications
- in-person interviews of USGS retired scientist Dr. Whitehead.

Blind Canyon Spring

The main spring area in Blind Canyon discharges at an elevation of 3,057 feet (GPS'd) and flows across the Q/T contact between the overlying Sand Springs Basalt (Covington and Weaver, 1991) and underlying Glenns Ferry Formation (GFF) deposited by Lake Idaho (Figure 11). Covington and Weaver (1991) at site #165-1 on their map show overlying cliff forming basalt as Sand Springs Basalt (Qss) with basal pillows then talus below it. The Idaho Geological Survey (IGS) (2005) mapped this same site as Flat Top Butte Basalt (Qftb) and underlying it are Tertiary Vent Deposits (Tvd?). No volcanic vent deposits were observed in this outcrop by the author. Hand samples collected by the author from the Tertiary outcrop show it is fossiliferous Glenns Ferry Formation (GFF) Lake Idaho flood plain units. The repetitious, upward fining olive-green silty clays are capped by carbonaceous brown paper shale directly comparable to typical characteristics at the Hagerman Fossil Beds National Monument. Previous geologic mapping by Covington and Weaver missed the GFF outcrop and IGS misidentified it as vent deposits and the outcrop wasn't exposed when Malde did his mapping.

A review of aerial photos shows this area was developed between the year 1985 and 1992. Roads were built and a water diversion trench was excavated to capture spring water. This exposed two new in-situ outcrops of GFF and associated Q/T contacts. Malde's 1971 map doesn't show this outcrop probably because at the time it was covered with slope overburden and vegetation as evident in air photos. An access road was constructed into Blind Canyon which exposed a high elevation (3,160 feet GPS'd) outcrop of GFF lake sediments located at -114.81801°, 42.69937° which is not recorded on geologic maps. This site represents the most southern in-situ outcrop of the GFF on the northside of the Snake River. These two recent exposures of the Tertiary sediments have helped define the geologic context of this spring area. The GFF outcrop forms the effective base of the East Snake Plain Aquifer at this spring with an elevation of 3,057 feet (GPS'd) and the GFF deposits may extend deeper by hundreds of feet.

Banbury Spring

The Q/T contact rises in elevation above the ESPA water table between Blind Canyon and Banbury Springs, then lowers in elevation again below the water table along the springs to the south side of Banbury. There are 2 wells (IDWR ID 316374 and 318398) that are located 1,200 feet south of Blind Canyon grade outcrop and 800 feet east from the Q/T contact mapped by IGS in 2005 and Covington and Weaver in 1991. The wells have been ground truthed with the owner for the location and well log then GPS'd. Both well logs describe approximately 40 feet of dense basalt overlying 50 feet of cinders then clay in the bottom 10 feet. This is consistent with outcrops along the Banbury Spring and Blind Canyon access road cuts where they exhibit pillows and breccia underneath a typical cliff forming competent but fractured Sand Springs basalt and underlying GFF.

Banbury Springs exhibits a linear elevated shelf feature that perches ESPA spring waters at an elevation ranging from 3,025 to 3,050 feet and creates a cascading water fall from this ledge. The springs and outcrop have a slight apparent southward dip and therefore more water issues from the south half of the spring than the north half of the spring. Whitehead (1992) in Plate #2 cross section #8 also shows a possible southward dip. Whitehead places most of the spring

discharge zone at approximately 3,000 feet elevation and slightly lower than the outcrop of Tertiary Basalt (Tb) on the southside of the spring. This is consistent with the authors field investigations.

Figure 12 shows a figure from Covington and Weaver (1991) which suggests a low elevation (2,900 feet) for the Quaternary/Tertiary contact (white dashed line) due to an ancient canyon filling process of 'cut and fill' and note the Sand Springs Basalt (Quaternary) filling a canyon cut into the Banbury (Tertiary) Basalt. Geologic samples inspected by the author from in-situ outcrops on the southside of the spring demonstrate a dense resistant thickness of clastic sediments, forming the horizontal base of the aquifer at approximately 3,050 feet. These sediments are exposed in outcrop on the northside of the Banbury spring from a road cut (Whitehead, 1992, Plate 2 Section #8) and on the southside below the diversion structure based on the authors field work. Field data suggests the contact is along the 3,025-3,050 foot level (yellow dashed line) rather than the 2,900 foot elevation (white dashed line) that Covington and Weaver show in Figure 12. The possible canyon filling volcanics likely extend down to approximately 3,050 foot elevation and dense sediments and tertiary basalt from 3,050 down to 2,900 feet or lower.

The higher elevation contact is more consistent with the character of the spring discharge and where outcrop samples were collected. In Covington and Weaver's (1991) cross section location 157-3 and the USGS topo map the springs are shown at the 3,050 foot; not 2,900 feet elevation as shown in the Figure 12. The south edge of Banbury Spring shows a clear boundary between the hydrophilic vegetation and desert species. This is due to an abrupt rise in the Q/T contact up to an elevation of 3,160 feet, as mapped by both Covington and Weaver (1991, Figure 12) and Whitehead (1992, Plate 2 section 8). The high elevation contact is above the water table and continues southward until dropping down again into Briggs spring. This area between the two springs has a high Q/T contact which correlates where the dye cloud split shown in Figure 14 and 15.

Briggs Spring

The Q/T contact drops at Briggs Spring from 3,160 feet down to an elevation of at least 3,015 feet based on Covington and Weaver (1991) and geologic samples collected during well drilling of a monitor well (IDWR well # 446314) located 500 feet north of the spring. The upper visible spring water was GPS'd at an elevation of 3,030 feet. The effective base of the ESPA at this spring is at least as deep as 3,015 feet based on the cuttings and geologic log from the monitor well. Large blocks of columnar basalt near the head of the spring that have been displaced from their original position on the cliff and rotated by 90 degrees through a toppling process. Columnar basalt is associated with pooling of lava in low depression areas which is consistent with a paleo canyon filling basalt. A nearby example is located four miles north of Briggs at the Stearns Spring canyon filling basalts which exhibit columnar features (Covington and Weaver, 1991, Figure 5).

3-D Quaternary Tertiary Geologic Contact Model

Numerous geologists have worked in this area on the spring hydrogeology since about year 1900 and recent work has added to this body of knowledge. The list below shows a long history of works with general dates of activity for some of the geologists:

- 1902 Israel Russell (USGS)
- 1927 O. Meinzer (USGS)
- 1936 Harold Stearns (USGS)
- 1963 Harold Malde, Howard Powers and Charles Marshall (USGS)
- 1970's Harold Malde and others (USGS)
- 1980 and 90's Harry Covington, Richard Whitehead, G.F. Lindholm (USGS)
- 2005 Virginia Gillerman, John Kauffman and Kurt Othberg (IGS)

Whitehead (1992) summarized numerous reports and this report provides a good source to find many of the reports. Surficial mapping has been refined through the years along with two important exploration wells that were drilled during the Regional Aquifer System Analysis (RASA) project (Lindholm, 1993).

Based on previous works, there are two main hydrogeological regimes that divide the aquifer into an upper level, high conductivity (K) layer and an underlying layer of low conductivity (Whitehead, 1992). Numerous reports also note the upper high K is dominantly Quaternary basalts exhibiting a high degree of fractures, flow contacts, conduits, pillows and associated breccia in the spring areas. The lower zone is of Tertiary age and numerous reports document this rock as low K consisting of larger columnar basalts, fewer fractures, secondary mineralization, clay rich lake sediments, and less frequent flow contacts (Lindholm, 1993; Whitehead, 1992). Lindholm (1993) also documents the upper 200 feet of basalts have a Specific Yield (Sy) range between 0.01 (1%) and 0.2 (20%) and lab tests of cores from INEL measured effective porosity from 4 to 22 percent (Johnson, 1965). Lindholm (1993) states that pillow features have the highest hydraulic conductivity values of the basalt rock types and that "…little has been done to define geologic controls on a local scale (pg. 10)" on the ESPA.

The Quaternary rocks in this area are composed of the Snake River Group and the Tertiary is composed of the Idaho Group (Lindholm, 1996). An undulatory erosional unconformity forms the contact between these rocks. The known vertical extent of the contact ranges over 1,000 feet from 2,538 feet elevation at Bancroft Spring outcrop up to 3,500 feet north of the city of Bliss. Malde (1991) notes that the contact in places is deeper than the modern-day canyon. Closer to the area of the Strickland trace, the vertical extent of outcrops range from a high of 3,212 feet at Clear Lakes Grade down to 2,885 feet at Blue Hart Springs (and likely lower than that) for a total of 327 feet of relief. According to Stearns (1936), ancient canyons of the ancestral Snake River, and other rivers, were filled by volcanic rocks from nearby shield volcano eruptions. Lava dams diverted river waters further to the south each time thereby cutting a new canyon, then the process would repeat again. Malde (1991) mapped the routes of the cut and fill sequence for these canyons.

A 3-D geologic contact model was built by the author to build upon earlier studies and "define geologic controls on a local scale" (Lindholm, 1993) by extending the subsurface geometry eastward from the spring areas. The basis of the model uses published map data, exploration borehole data from Harold Malde (1971 & 1972), Covington and Weaver (1990 & 1991), Idaho Geological Survey (2005), Whitehead (1992), Lindholm (1993 & 1996). These publications provide 124 outcrop and 3 well logs control points and are shown on Figure 13 as light blue/teal colored dot symbols. The remaining 226 control points (black dot symbols) are sourced from ground truthed well drilling logs, new outcrop mapping by the authors, and GPS'd elevations of spring level controls. The total area of the model covers 465 square miles and includes the color zones shown in Figure 13. The model was developed using Kriging method in Surfer® (Golden Software, LLC) version 23.2.176. The colored elevation zones illustrate how the contact undulates with some low areas correlating to the buried canyons mapped by Malde (1991, Figure 11 on page 274). The area of interest for this report is shown as a red colored dashed square in Figure 13.

Figure 14 shows the QT contact surface near the Strickland Trace extending north to Malad Gorge. Near the Malad Gorge, the Victor Trace, which was completed in year 2014, is labeled and shown as a green colored 3-D polygon. For scale, the trace extended for 3.1 miles distance and followed Malde's (1991) buried canyon #2 route. The contour lines for the QT contact are 5 foot intervals and the vertical exaggeration is 10x. Black dots are control points and most of them along the south and west boundary are not visible due to the view angle. The Strickland Trace flow path is labeled and displayed as a 3-D surface colored bright green in Figure 14. The upper surface of the Strickland Trace polygon shown on Figure 15 is the same as the high resolution 2013 water table map and the sides or walls extend down to the QT contact surface for reference. The trace flow path follows the groundwater gradient at right angles (Mundorf, 1964 p.143 & 195) with a single peak breakthrough curve, thereby supporting a homogenous aquifer response at this scale. A similar response has been shown at the Mile Post 31 tracer test located to the northeast of the Strickland trace and single peak breakthrough curves supporting a homogenous aquifer response at that scale (Farmer and Blew, 2022). Single peak breakthrough curves are the most common pattern in all the traces to date on the East Snake Plain Aquifer.

Note the area in Figure 14 where the dye cloud splits and flows into Banbury and Briggs Springs. This area is mapped with a high elevation QT contact (3,160 ft) that rises above the water table shown in Figure 15 in the lower left corner. Three well logs near the dye divergent area, (IDWR wells #461696, 420549, 387026) encountered clay at an elevation ranging from 3100 to 3125 feet on down to approximately 2998 feet or the depth of the well. Figure 15 also shows the year 2013 water table splitting at this same location and steep groundwater gradients occurring around the spring discharge areas. The water table flattens between the dye injection well and the springs possibly due to a 'bench' feature in the subsurface as exhibited in outcrop at Banbury spring.

Figure 16 illustrates the saturated thickness of the high K portion of the aquifer within the Quaternary Basalts. Aquifer thickness was calculated in Surfer by developing an isochore map

between the 2013 water table elevations and the QT contact. Contour intervals are 5 feet and the map shows a thinning of the high K aquifer saturated thickness as it approaches the spring areas. Thinning is likely due to the steepening water table gradients near the aquifer discharge areas. There is still water present within the underlying low K Tertiary rocks but the fractures are tight and commonly mineralized with fewer flow contacts (Lindholm, 1993). When the low K Tertiary rocks outcrop either infrequent seeps or no springs are present, therefore, the QT contact appears to form the effective base of the ESPA in this area.

The depth to water in the Strickland well was measured at 62 feet and the total depth of the well is 123 feet which equates to a saturated thickness of 61 feet in the well. The QT contact and water table map did not use the Strickland well in the modeling as the well does not penetrate the QT contact. The isochore model shows the saturated thickness of the aquifer at this well location should be 65 feet. The observed verses the modeled values appear to correlate to within 4 feet but the well terminated in rubbly and bulbous basalt and therefore it did not encounter a low K geologic formation to confirm this point of contact. The isochore thickness map (Figure 16) represents a modeled surface for the saturated thickness of the aquifer within the Snake River Group Quaternary Basalts.

The rock units modeled and described in this report are the same units described by Lindholm (1993, pg. 51 and Figure 37) where high K Quaternary rocks make up layers #1 and #2; and low K Tertiary rocks make up layers #3 and #4 in a multi-layer numerical groundwater model.

Dye Flow Path Discussion

Tracing on the ESPA in fractured basalt requires flexibility in the spatial and temporal extent of sampling. Prior to initiating the trace, local groundwater data (Figure 3) was used to help determine possible locations of dye emergence. The groundwater potentiometric maps, while detailed, did not provide adequate resolution for determining the emergence areas of dye. Specific conductivity data collected during a 2011 synoptic survey (Farmer & Blew, 2014b) indicates a correlation where the dye flowed. Low (1987) and Baldwin and others (2006) described a change in specific conductance of groundwater on the ESPA. In general, specific conductance decreases from south to north on the western edge of the ESPA. In the study conducted by Baldwin et al (2006) a line was identified, generally running east to west, in which the aquifer north of the line has a specific conductance of <500 µS/cm and south of the line is >500 µS/cm**.** Baldwin (et al, 2006) used specific conductance, stable isotope and nitrate-nitrogen (NO_3-N) data to delineate the apparent separation of two flow systems based on chemical signature (Figure 17).

In a 2011 synoptic survey of the west edge of the ESPA, groundwater elevations and specific conductance were measured at select wells. This data generally aligns with the data reported by Baldwin et al (2006). The specific conductivity data provides evidence that dye emergence areas would be different than those identified using the potentiometric maps and GIS Steepest Path tool. Potentiometric data indicated a general southwest groundwater flow. The conductance data indicate a general east to west flow of groundwater in the area (Figure 18). Based on this chemical data, dye emergent areas would have been in the Briggs and/or Banbury

area and not the Clear Lakes Springs area. The data for specific conductivity reported by Farmer and Blew (2014b) support data reported by Baldwin et al (2006) as well as Mann and Low (1994), Clark and Ott (1996) and Schorzman et al (2009). These data sets provide insights into understanding water movement in the ESPA and may guide future studies.

Groundwater Velocity

The groundwater velocities for the Strickland trace can be found in Table 6. Dominant velocity is calculated as the time from dye injection to the peak concentration of dye. Groundwater velocities from the Strickland well to Briggs Springs and Banbury Springs are within the range determined from other groundwater tracer tests on the ESPA as shown in Figure 19 (Farmer & Blew, 2009, 2010, 2011, 2012, 2014a; Farmer et al., 2014b, and Farmer and Blew, unpublished data). Figure 19 shows the general proportional linear relation between the gradient and dominant velocity for traces completed on the lower basin ESPA by Farmer and Blew. Meinzer (1934 and 1942) published that if groundwater flow is laminar, then velocity is directly proportional to hydraulic gradient and it conforms to Darcy's Law. Velocities are not likely constant throughout the flow path and gradients generally steepen in the near rim areas which are largely driven by hydraulic conductivity and the elevation of spring discharge. Based on previous tracer studies on the lower basin ESPA (Farmer & Blew, 2009, 2010, 2011, 2012, 2014a; Farmer et al., 2014b, and Farmer and Blew, unpublished data), groundwater velocities appear to increase in the near spring areas and are 3 to 10 times faster than the 100 to 150 ft/day reported by Baldwin (2006, p.15).

The lower basin ESPA tracer tests also show a strong correlation between dominate velocity and trace distance (Figure 20). These traces all followed similar flow paths with varying distances from the dye emergent springs. Not only did the distance change, but the hydraulic gradient decreased as distance increased. The Meyers and Victor traces near the Malad Gorge were the two longest traces completed in that area with dominant velocities of 541 ft/day and 212 ft/day respectively. The Hopper trace was 5,490 feet which is approximately half the distance of the Meyers trace of 11,900 feet and a third of the distance of the Victor trace or 16,350 feet. The Hopper trace had a dominant velocity of 948 feet, nearly twice the velocity of the Meyers trace. In comparison, four wells monitored for the Mile Post 31 trace (Farmer and Blew unpublished data) were over 40,000 feet from the dye injection point and dominant velocities range from 256 - 419 ft/day. Despite a longer flow path, the velocities recorded for the Mile Post 31 trace are not substantially different from the Meyers and Victor trace. The Strickland trace, at over 18,000 feet, had dominant velocities of just over 400 ft/day which are comparable to the Mile Post 31 trace. Based on dominant trace velocities, the groundwater velocities on the western portion of the ESPA are generally between 250 ft/day and 400 ft/day except close to (within about 2 miles) spring areas where they can increase to 1,000 to 2,000 ft/day range. Baldwin (2006) reports calculated velocities using Garabedian (1992) methods of 100 to 150 ft/day. Modeling is underestimating aquifer velocities and therefore the conductive nature of the aquifer.

Reynolds and Peclet Numbers

Geology of the western third of the ESPA consists of multiple basalt layers including zones of highly fractured basalt. Based on the results of the tracer study, groundwater velocities are higher than those typically found in aquifers with matrix of silt, sand, or gravel. As the velocity of groundwater increases, the inertial forces of water begin to overcome the viscous forces (Fetter, 1988) and in groundwater flow turbulence begins to develop. As the inertial forces predominant, aquifer flow begins to transition from laminar to turbulent flow (Bear, 1972). The Reynolds Number (Re) provides a measure of the ratio between the viscous forces and inertial forces of water. Authors provide a range of where turbulent flows begin, however flows with a R*e* in excess of 2000, are generally considered turbulent (Fetter 1988, Bear 1972).

Dacry's Law is the guiding equation for determining flow within most aquifers. It specifies a linear relationship between specific discharge and hydraulic gradient. At critical velocities and flow apertures, water molecules in the aquifer no longer move in parallel streamlines (Fetter, 1988) and the linear Dacry relationships begin to collapse. Bear (1972) and Fetter (1988) indicate this transition to nonlinearity to be between Re of 1 to 10. Within this transition zone, flow is not considered turbulent but is likely nonlaminar. Using computation fluid dynamics to simulate a porous media (sphere size 10-3 m), Chaudhary et al (2011) found deviations from Darcy as flows increased and Re exceeded 1. Wang et al (2019), in a laboratory column study of sands and silts found the critical Re to be "infinitely close to zero, which is inconsistent with Bear's" critical Re of 1 – 10.

The critical Re for aquifers with fractured matrix may be different than those reported for porous media. The change in the viscous forces and inertial forces occur on the boundary layer. Therefore, the scale of the system being evaluated must be considered when assessing the impact of Re. For example, in pipe flow, laminar conditions persist until Re>2100 (Bear 1972). Ji et al (2008) study the movement of DNAPL migration in roughed walled fractures. The fractures they study had an estimated hydraulic aperture ranging from 612 to 713 μm and at Re=10 there is a 10 % deviation from linearity and Re=50 the deviation from linearity was 30%. The fracture apertures study by Ji et al (2008) are several orders of magnitude smaller than those found on the ESPA. Factors that impact Re in fractured flow include the diameter of the aperture, roughness of the fracture, sharp corners, tortuosity, and other fracture characteristics. Javadi et al (2014) states "the critical Reynolds number is closely dependent to geometrical attributes of fracture (such as contact ratio, relative roughness, aperture, and matedness), and easily changes dramatically with variation of such attributes."

Despite the foregoing discussion and the complicated issues associated with Re in fractured aquifers, it does provide a first cut at beginning to understand the nature of flow on the ESPA. It is important for modeling and forecasting to understand if the flow within ESPA is linear or nonlinear. Based on the measured velocities from this tracer study, understanding the scale at which the linearity is measured should also be determined. This tracer study, and other completed on the ESPA and the analysis of Re, provide motivation for additional investigation into the nature of flow on the ESPA.

Re is calculated using the formula:

$$R_e = \frac{\rho v d}{\mu}$$

where

Re = Reynolds Number
ρ = the fluid density
v = discharge velocity
d = diameter of the flow passage
μ = fluid viscosity

Worthington and Soley (2017) describe the use of trace velocity as one method for determining Re. Their method includes the calculation of the flow area aperture in a carbonate aquifer. Data does not exist for the ESPA to allow for the calculation of the flow area aperture so Re are calculated based on a continuum of aperture sizes (Figure 21). Figure 21 used dominant groundwater flow velocities from tracer tests to calculate Reynolds numbers. Shorter distance-fast velocity traces plot on the left side and longer distant-slower velocity traces on the right side with the Strickland trace being central. Dominant velocity of the Strickland trace indicates that if the flow area aperture is greater than 0.3 inches the Re will exceed a threshold of 10. It is likely that the aperture is at least one order of magnitude large than 0.3 inches.

Related to Re is the Peclet Number (Pe) which provides a measure of the aquifer forces with regards to the movement of dye and is the ratio of the advective forces to the diffusive forces. Pe is calculated as

$$p_e = \frac{Lu}{D}$$

where

Pe = Peclet Number
u = discharge velocity
L = characteristic length
D = diffusion coefficient

Due to the nature of the ESPA, the characteristic length (L) is unknown and like the Re the Pe is reported as a range based of varying L. Doummar et al (2010) reports that a Pe >6 is an indicator that advective forces are the primary forces responsible for dye movement. Various diffusion coefficients for sodium fluorescein have been reported and range from 4.9E-10 to 6.48E-10 (Olsson and Grathwohl 2007, Casalini et al 2011, Ruiz 2017). The calculations here a D of 6.48E-10 was used. Figure X shows the results of the Pe calculations. Based on the calculations and the general velocities recorded, movement of dye is dominated by advective forces.

Conclusions

The first trace at a location typically produces coarse data that shows general groundwater direction and velocity for refinement and preparation for a second trace. The Strickland trace is no exception to this, and a second trace is recommended to improve results. This trace presented a number of logistical and technical challenges. The trace did not follow the modeled dye path necessitating an adaptive response to expand the study area. These factors also provided the motivation to explore other data sources for predicting dye flow path directions such as water chemistry. If a second trace is performed, it is recommended that the mass of dye be tripled from 6 pounds to approximately 20 pounds based on peak results of other traces. Most of the dye traces that have been performed since year 2009, should have had roughly twice as much dye released to increase peak concentrations from weak signals on the order of 0.1 ppb up to a discernable value of 1.0 ppb. Low concentrations cause stepped data as shown in Figure 10 for Briggs spring. A concentration of 1.0 ppb is 10 times below the aesthetics based recommended value of 10.0 ppb for Fluorescein (Wilson, 1986) and by ANSI/National Standard 60 for use in drinking water.

The results of this trace are consistent with other traces that have been completed on the western ESPA. The main exception is the dye cloud split and flowed into the edges of Briggs Spring and Banbury spring; likely due to a high elevation Quaternary Tertiary geologic contact that wedges eastward into the aquifer. The maximum velocity to Briggs was calculated at 700 ft/day and Banbury south side at 706 ft/day. The dominant velocity was calculated at 404 ft/day to Briggs and 427 ft./day to Banbury south side. These values should be rounded for significant figures. The interpolated dominant velocity from well to well (Strickland to Mink Farm) was 600 ft/day.

Dye tracing provide empirical direct data for flow paths which can bolster indirect inferred flow paths from reports by Baldwin et al (2006), Mann and Low (1994), Clark and Ott (1996) and Schorzman et al (2009). High groundwater velocities provide evidence that the movement of dye within the aquifer is dominantly driven by advective forces and diffusive forces are minimal. The Reynolds number graph indicates non-laminar flow may occur at aperture sizes larger than about 1 inch. Figure 19 shows a proportional relation between velocity and gradient and therefore suggesting it meets Darcy.

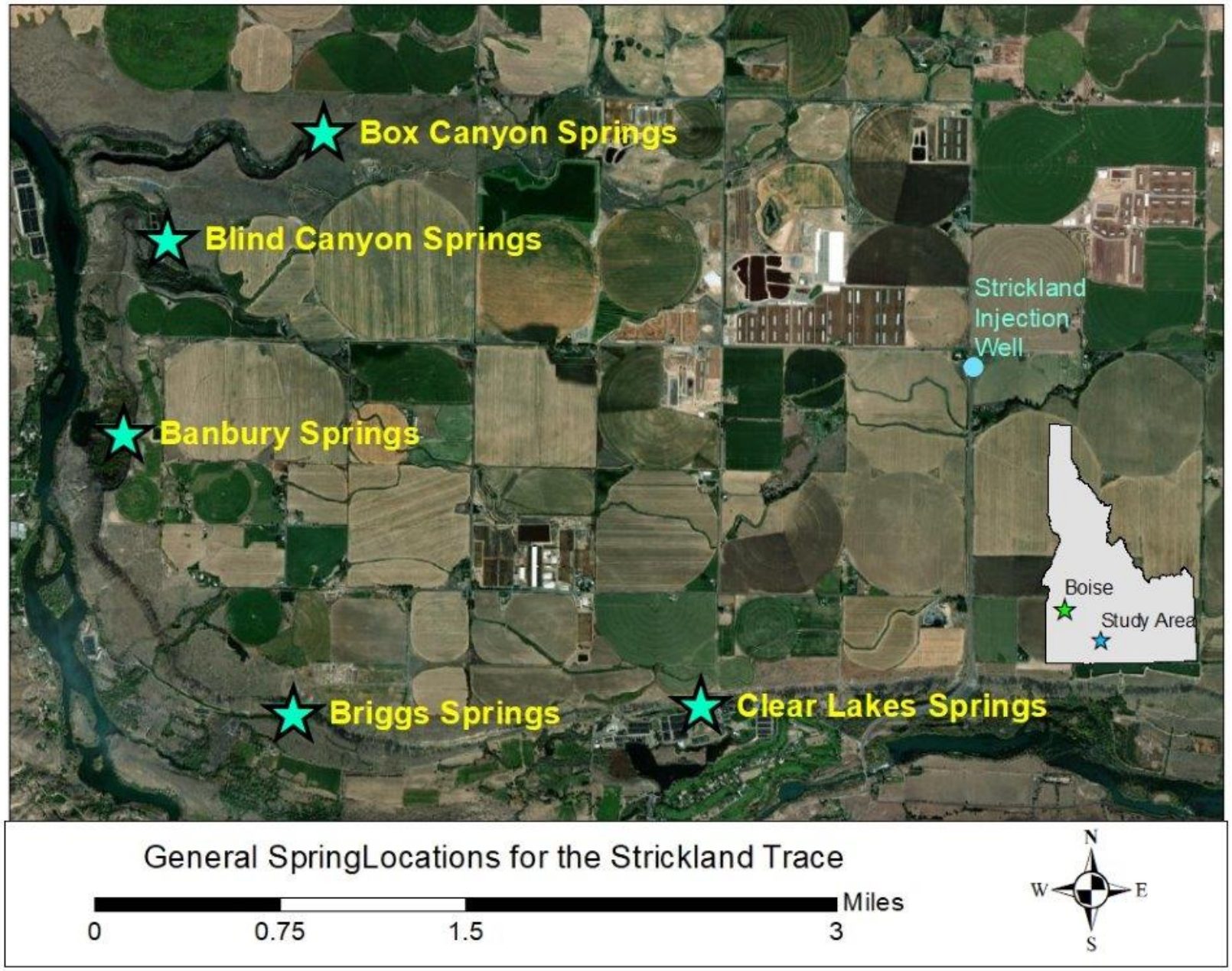

Figure 1. Location of springs within the Strickland trace study area.

Figure 2. Cavernous basalt in the Strickland well below the pump base, which is seen along bottom edge of image. This is a 6-inch diameter borehole for scale.

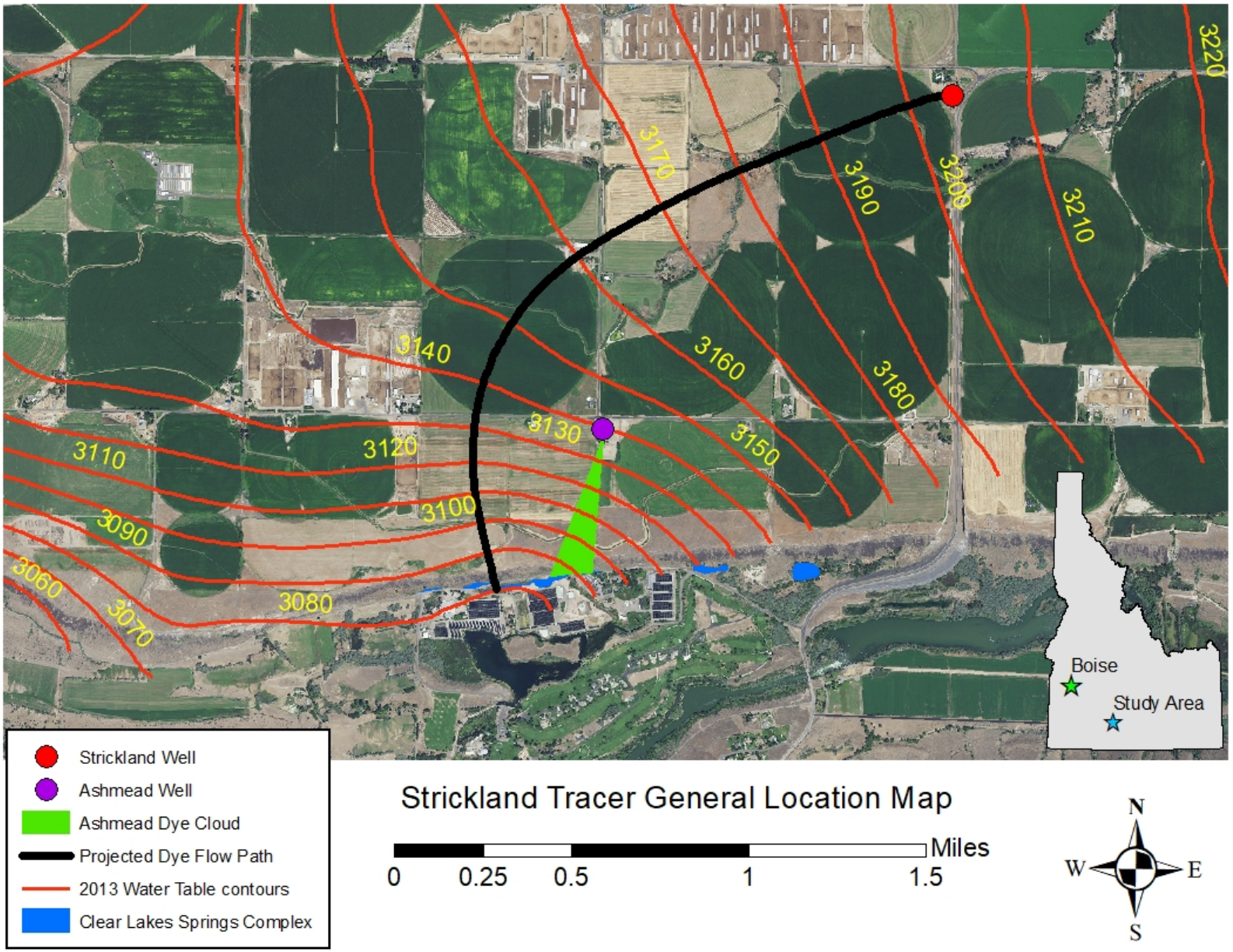

Figure 3. Location map of the Strickland trace model prediction for possible dye flow path (black line) based on the 2013 water table grid and GIS 'Steepest Path' tool.

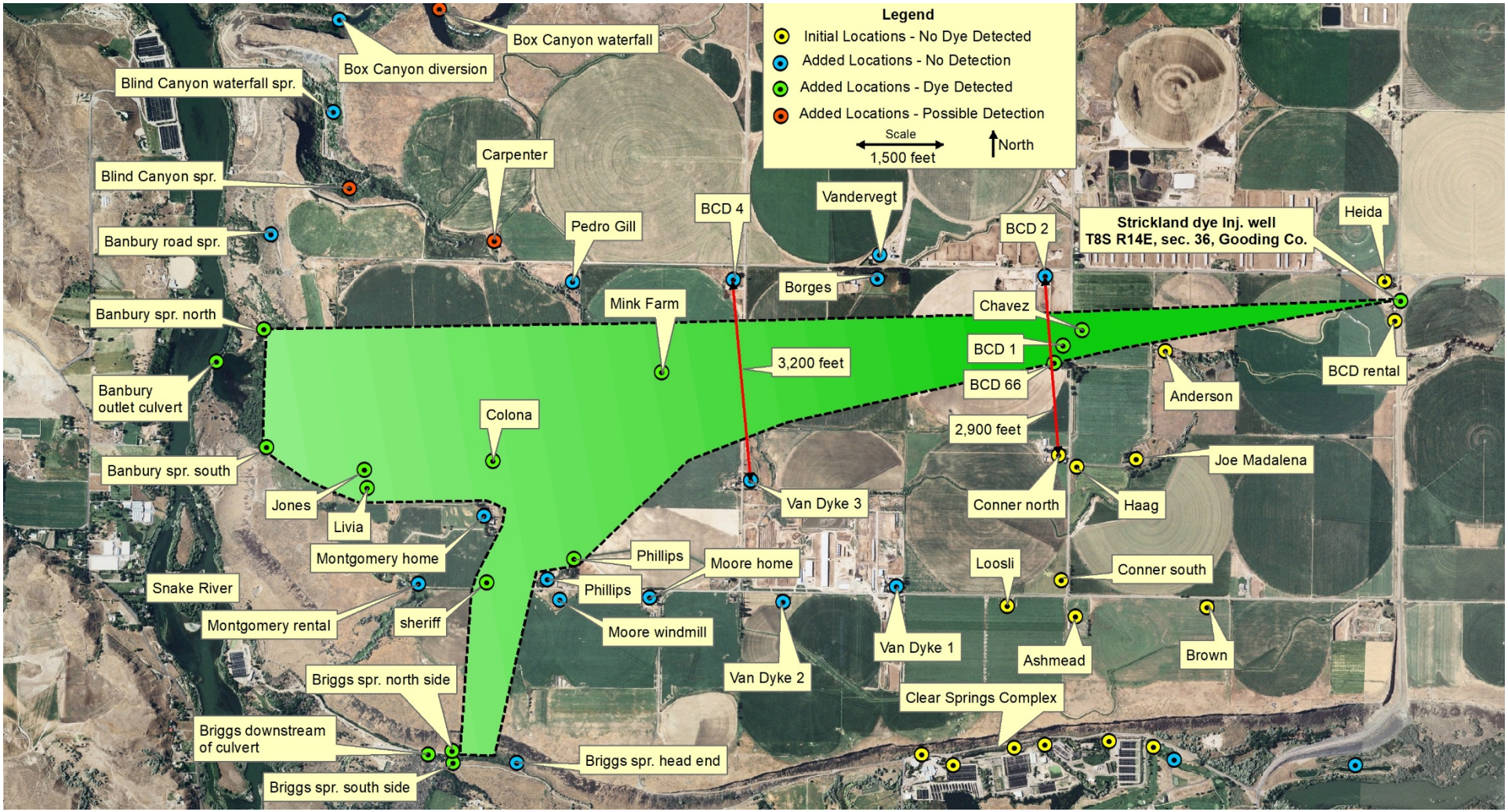

Figure 4. Monitoring locations and estimated dye flow path for the Strickland trace.

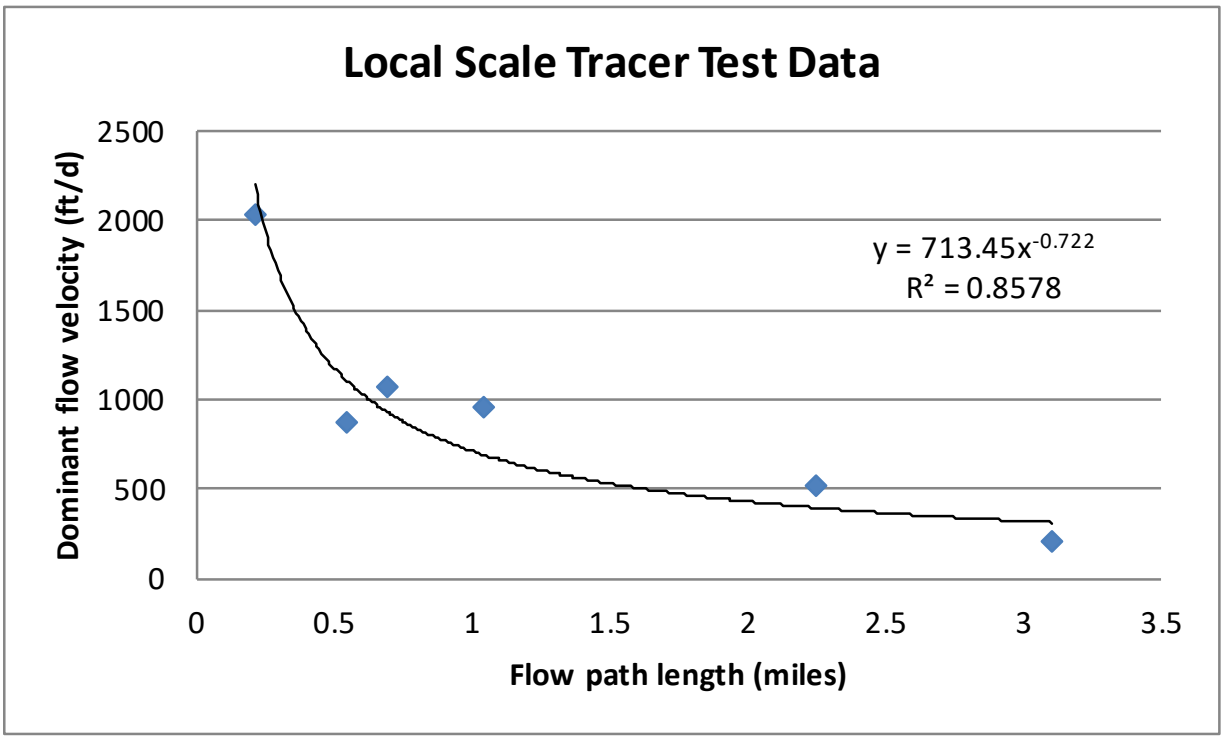

Figure 5. Groundwater flow velocity versus flow path length for six tracer tests conducted on the western portion of the ESPA.

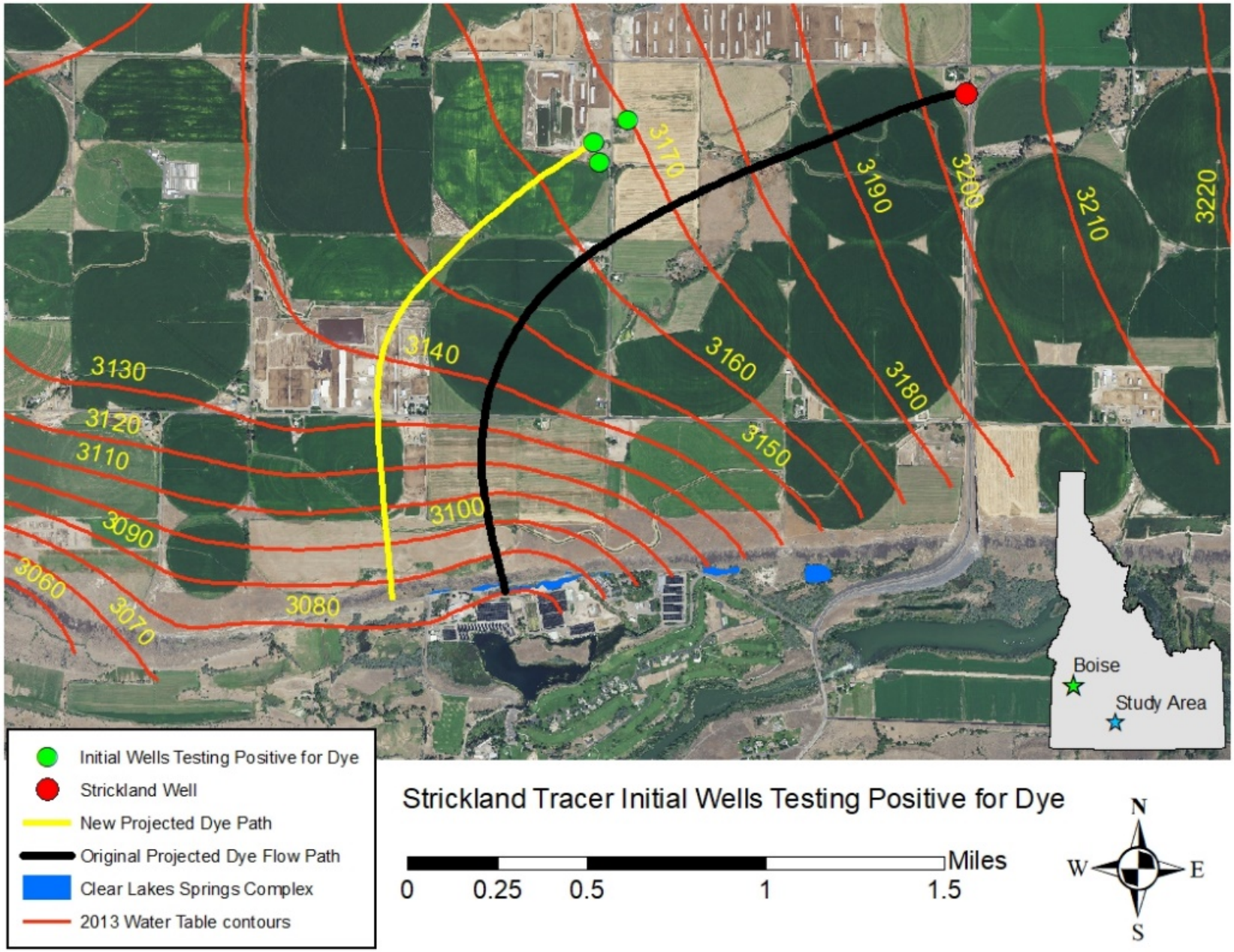

Figure 6. Initial wells testing positive for dye with GIS 'Steepest Path" tool applied resulting in the predicted yellow line flow path.

Trace	Longitudinal Distance (miles)	Lateral Spread Interpolated (miles)	Calculated Ratio	Normalized Ratio
Strickland	1.1	.28	.25	3:0.75
Shoshone	3.2	1.6	.5	3:1.5
MP 31	8.5	4.5	.5	3:1.5

Table 1. Comparison of Interpolated Transverse Dispersion to Dye Flow Path Longitudinal Distance.

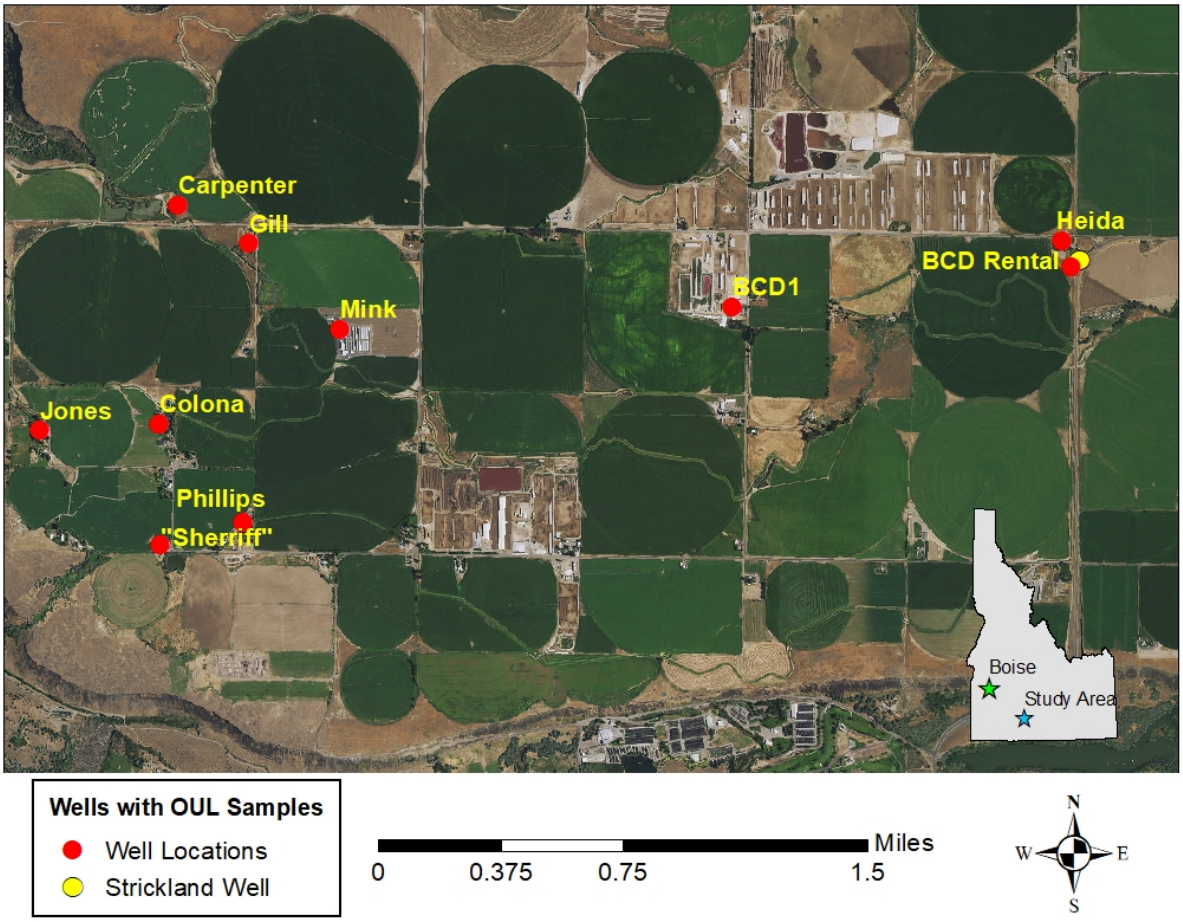

Figure 7. Strickland Trace wells that had samples collected for laboratory analysis.

Date	Location	Lab Results (ppb FL)
11/15/2013	Heida	ND
11/15/2013	Strickland	ND
11/15/2013	BCD Rental	ND
11/25/2013	BCD 1	1.270
12/4/2013	Mink	0.094
12/6/2013	Mink	0.076
12/8/2013	Colona	0.119
12/10/2013	Philips	0.206
12/13/2013	Sheriff	0.031
12/16/2013	Jones	0.104
12/27/2013	Colona	0.192
12/27/2013	Carpenter	0.013
12/27/2013	Gill	ND
1/17/2014	Carpenter	ND
1/17/2013	Gill	ND

Table 2. Results of laboratory analysis for water samples collected at well monitoring sites.

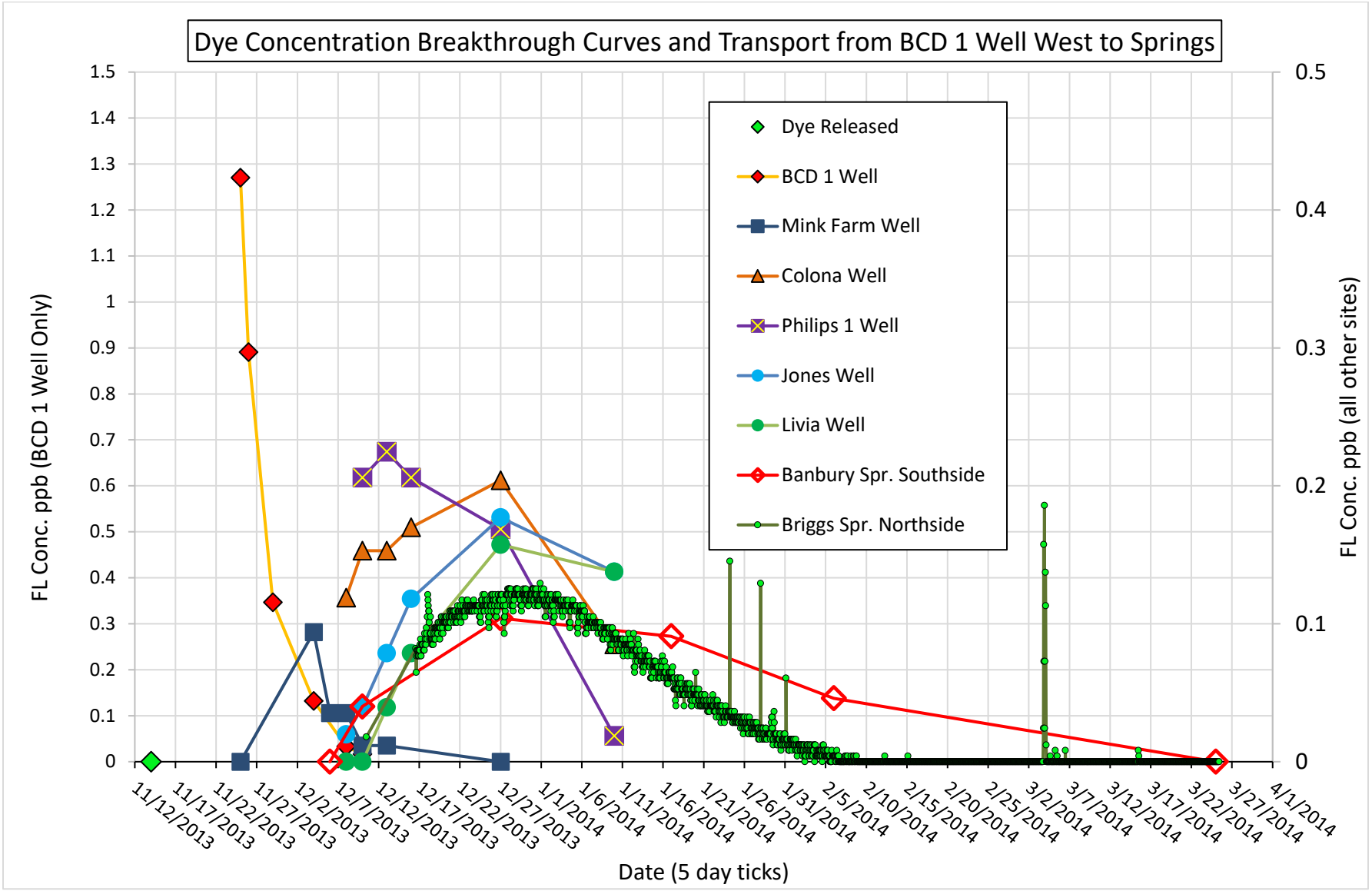

Figure 8. Dye breakthrough curves for wells and springs along the flow path. Field measurements of dye concentrations in water were calibrated to grab water sample results from the lab. For graph clarity purposes, only the BCD 1 well data is plotted on the left vertical axis.

Date	Location	Concentration (ppb)
12/10/2013	USGS Gage Northside	0.018
12/10/2013	USGS Gage Southside	0.040
12/16/2013	USGS Gage Northside	0.082
12/27/2013	USGS Gage Northside	0.105
12/27/2013	Downstream Diversion	0.067
1/10/2014	USGS Gage Northside	0.094
1/17/2014	Spring Head	ND
2/6/2014	USGS Gage Northside	0.020
3/25/2014	USGS Gage Northside	ND

Table 3. Laboratory results for water samples at Briggs Springs area.

Dye Packet Results Briggs Springs				
Location	Placed	Retrieved	Duration (days)	Concentration (ppb)
Briggs Springs North Side of Channel	12/15/2013	3/25/2014	100	44.7
Briggs Springs South Side of Channel	12/1/2013	3/25/2014	114	5.8

Table 4. Laboratory results for charcoal samplers at Briggs Springs.

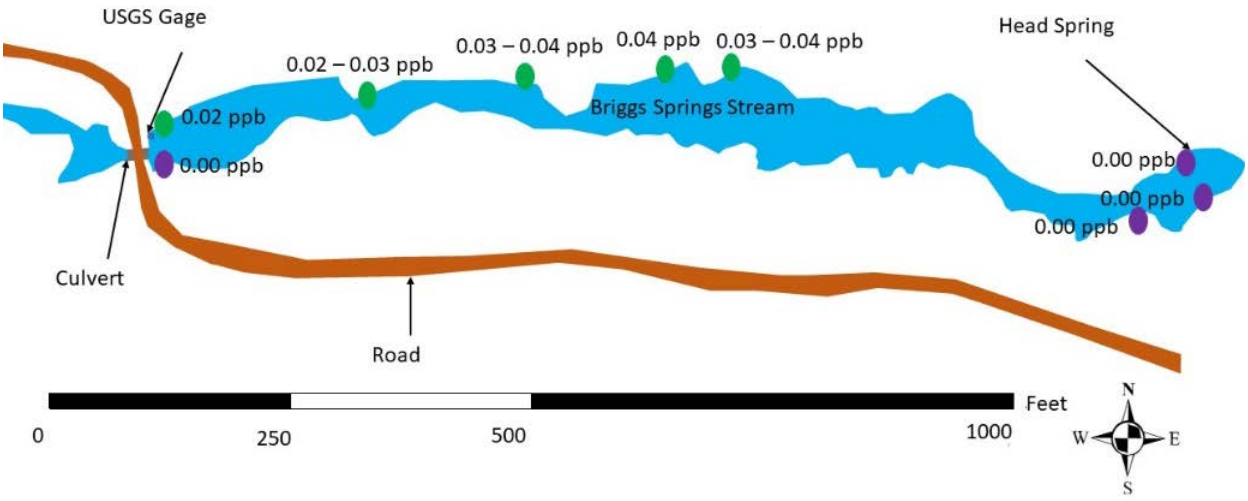

Figure 9. Field testing results using a submersible fluorometer at Briggs Springs on 1/17/2014.

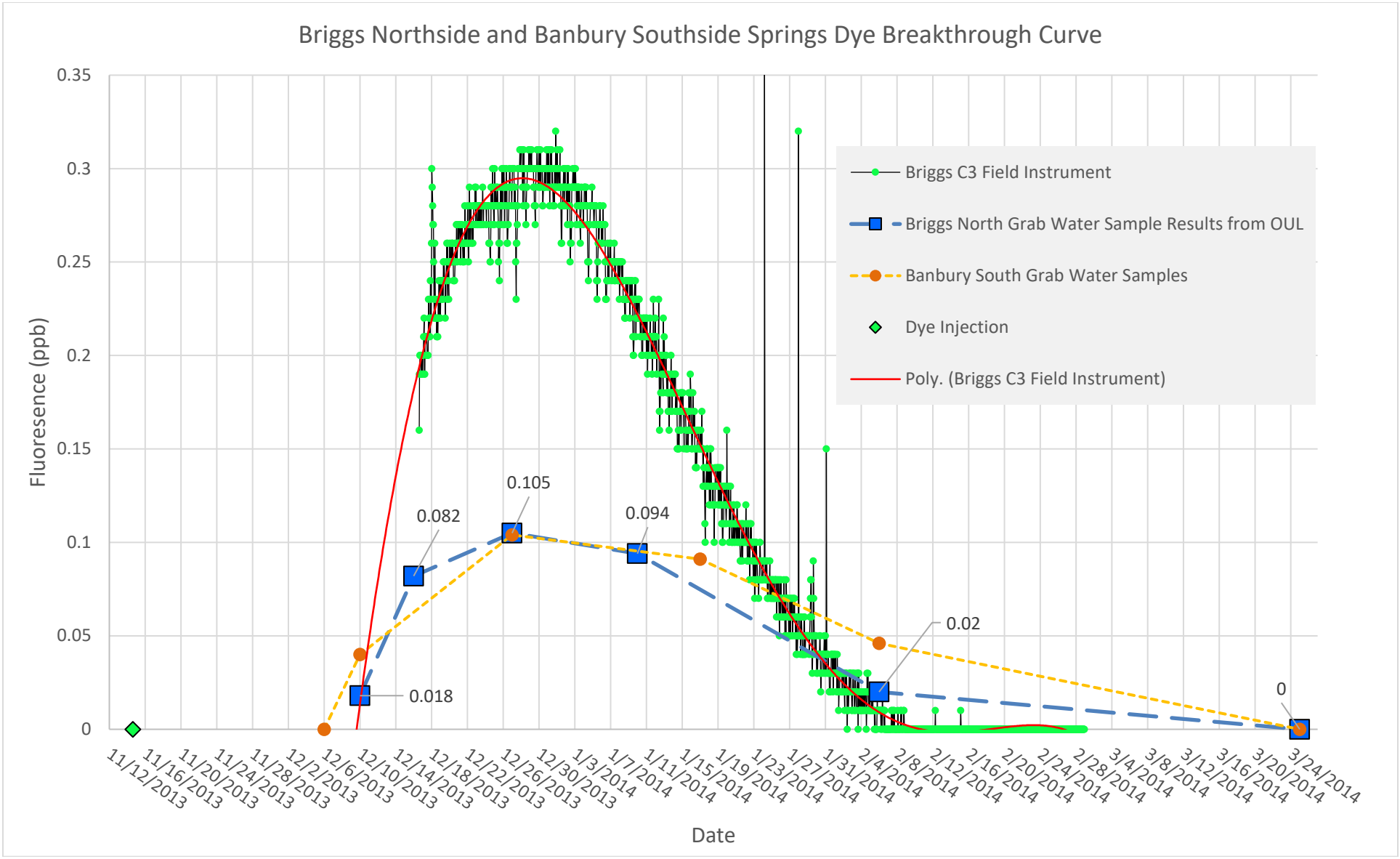

Figure 70. Dye concentrations measured in Briggs Springs near the USGS Gage. Green data represents concentration measured with a submersible fluorometer. Blue squares and orange circles are grab water samples analyzed by OUL.

Date	Location	Concentration of Dye (ppb)
12/6/2013	Banbury Road Spring	ND
12/6/2013	Morgan Lake Discharge	ND
12/6/2013	Banbury South	ND
12/10/2013	Banbruy South	0.040
12/13/2013	Morgan Lake Discharge	0.012
12/27/2013	Banbury Road Spring	ND
12/27/2013	Banbury South	0.104
12/27/2013	Morgan Lake Discharge	0.046
12/27/2013	Banbury North	ND
1/17/2014	Banbruy South	0.091
1/17/2014	Banbury North	ND
1/17/2014	Morgan Lake Discharge	0.024
2/6/2014	Banbury South	0.046
3/25/2014	Banbury South	ND

Table 1. Laboratory results of water samples from the Banbury Springs Complex.

Spring	Maximum	Dominant
Briggs	700	404
Banbury	706	427

Table 2. Groundwater velocities from the Strickland well to the Briggs and Banbury Springs in feet per day.

Dye Packet Results Banbury Springs				
Location	Placed	Retrieved	Duration (days)	Concentration of dye (ppb)
Banbury South	12/1/2013	3/25/2014	115	119.0
Banbury North	12/1/2013	3/25/2014	115	1.89

Table 3. Laboratory results of charcoal samplers from Banbury Springs monitoring sites.

Date	Location	Dye Concentration (ppb)
12/10/2013	Blind Canyon Creek	0.021
12/10/2013	Box Canyon Diversion	ND
12/27/2013	Gill well	ND
12/27/2013	Carpenter well	0.013
1/17/2014	Blind Canyon Spring	ND
1/17/2014	Blind Canyon Road Spr.	ND
1/17/2014	Gill well	ND
1/17/2014	Box Canyon Diversion	ND
1/17/2014	Carpenter well	ND
1/17/2014	J Canal water	ND

Table 8. Laboratory results of water samples from the Blind and Box Canyon areas.

Location	Date Placed	Date Retrieved	Duration (days)	Concentration (ppb)
Box Canyon Spring	12/1/2013	3/25/2014	115	0.375
Box Canyon Diversion	12/1/2013	3/25/2014	115	ND

Table 9. Laboratory results of charcoal samplers from the Blind Canyon and Box Canyon Springs area.

Figure 11. Outcrop of Tertiary Glenns Ferry Fm. clay rich sediments with fossil bivalves which forms the effective base of the East Snake Plain Aquifer at 3,057 feet elevation. The overlying quaternary basalt exhibits basal pillows. (photos by David Blew)

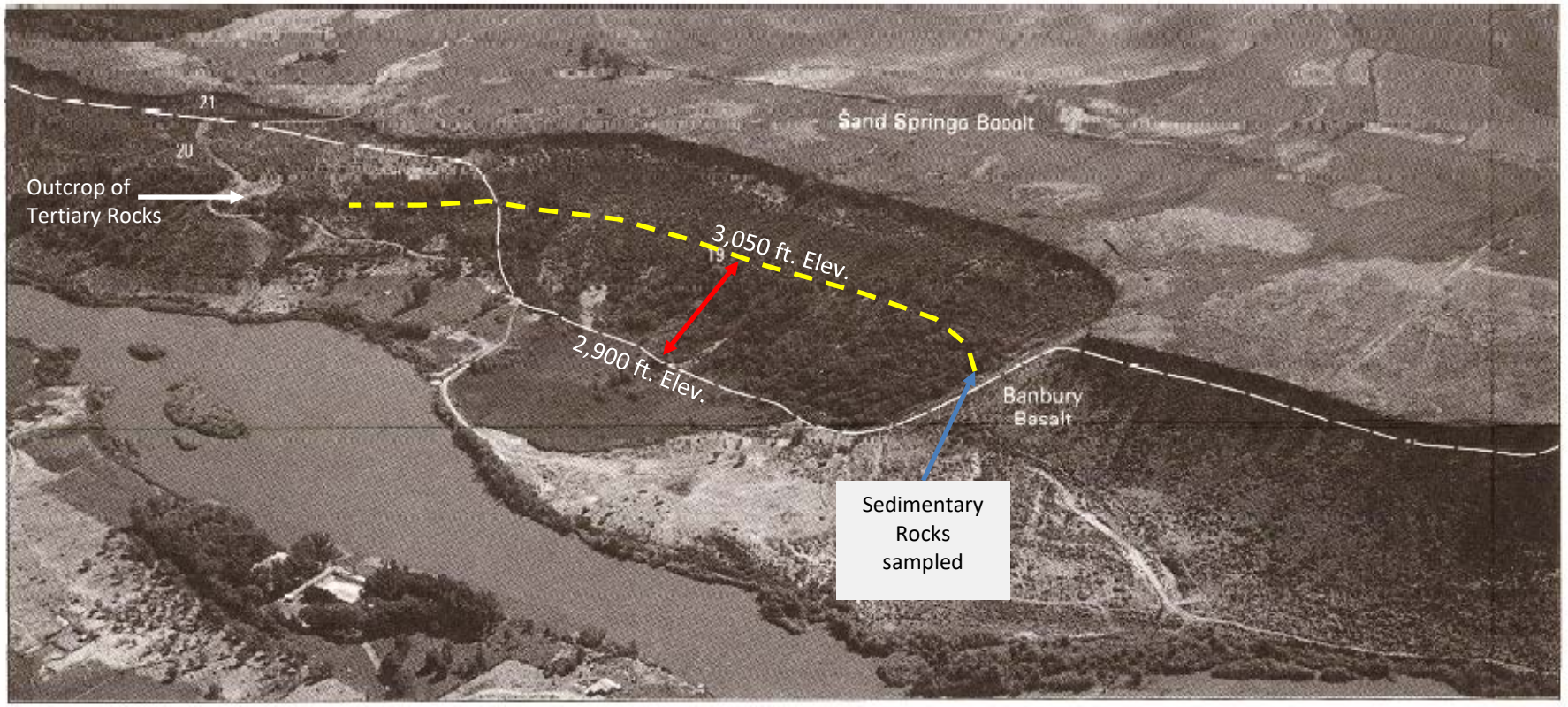

Figure 6. Banbury Springs. Springs emerge from pillow lavas of the Sand Springs Basalt that fill a tributary canyon of an ancestral Snake River canyon. Dashed lines indicate approximate location of wall of ancestral tributary canyon incised into Banbury Basalt. Numbers correspond to spring locations.

GEOLOGIC MAPS AND PROFILES OF THE NORTH WALL OF THE SNAKE RIVER CANYON, THOUSAND SPRINGS AND NIAGARA SPRINGS QUADRANGLES, IDAHO

By

H. R. Covington and J. N. Weaver

1991

Figure 12. Modified from Covington and Weaver (1991) to show outcrops of Tertiary rocks on both the north and south side of the Banbury spring which are at the same elevation as the effective base of the ESPA spring discharge horizon shown with yellow dashed line at 3,025 to 3,050 feet. Covington and Weaver show the depth of the ancestral canyon as the white dashed line at an elevation of approximately 2,900 feet but this appears to be inconsistent with field observations.

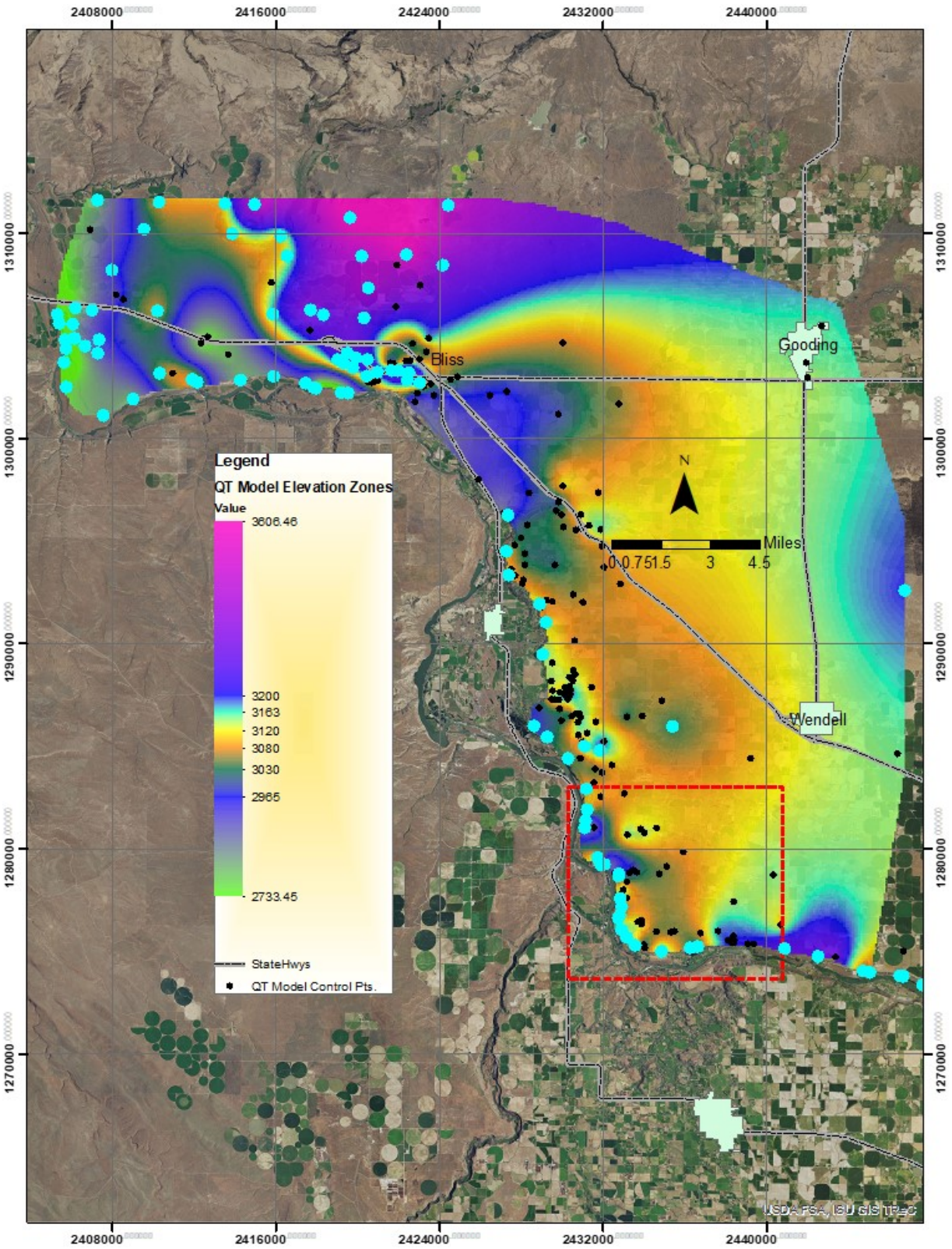

Figure 13. Area and elevation zones in feet units of the 3-D Model for geologic contact between the overlying high 'K' Quaternary and underlying low 'K' Tertiary rocks. Red dashed square is the area of interest for this report. Coordinates are in IDTM. Teal colored dots are control points sourced from publications.

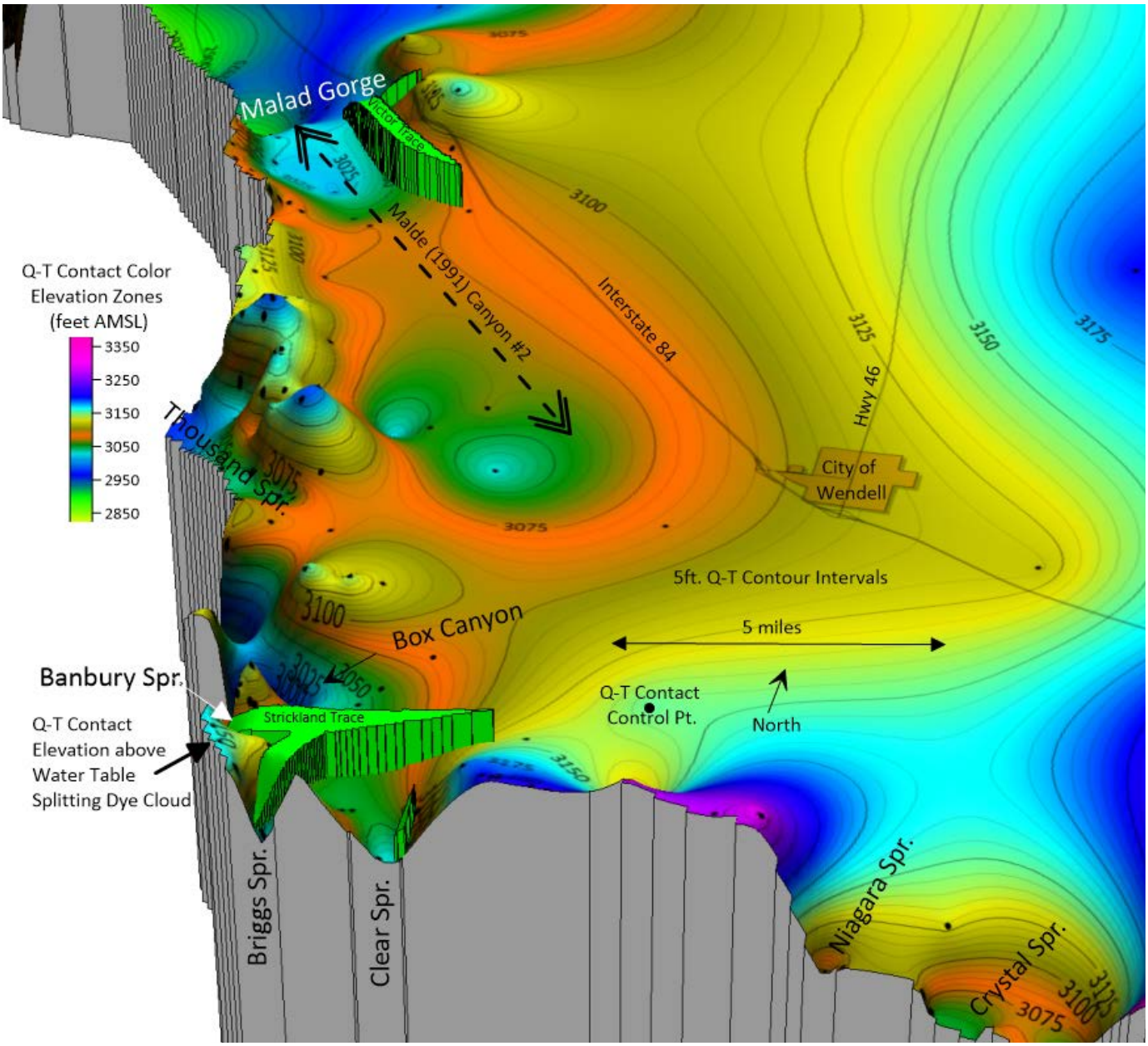

Figure 14. 3-D perspective model with a 10x vertical exageration of the geologic contact between the overlying Quaternary high K basalts and underlying low K Tertiary rocks creating the effective base of the ESPA in this area. The Q-T contact rises above the water table between Briggs Spring and Banbury Spring creating a low K eastward extending 'wedge' feature splitting the dye cloud into each spring. Conversley, the Victor Trace to the north, followed Malde's Canyon #2 (1991) and was constrained by convergent flow paths into Malad Gorge. The control point in the upper right corner is defined by Whitehead (1992) pg. B9 Figure 4. The perimeter control points are from USGS and IGS maps. The interior control points are from ground truthed well drilling logs.

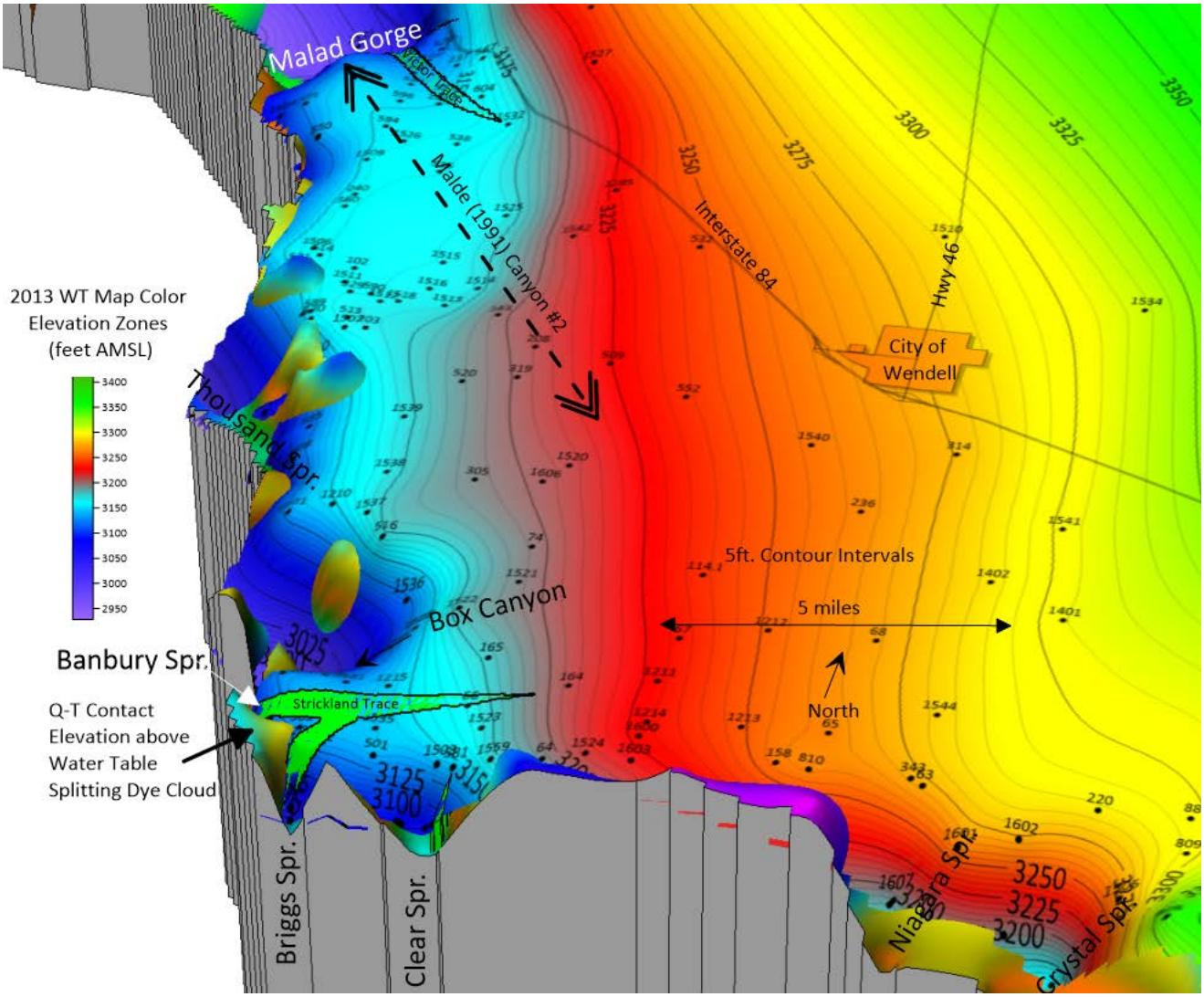

Figure 15. Year 2013 high resolution water table map shown with color zones and 5 foot contour lines. Water level control points and ID# are displayed as black dots. Note how the Q-T contact rises (shown with teal, green, and tan color zones) above the water table elevation (shown with navy blue color zone and contour lines) at the location where the dye cloud split into the Banbury and Briggs springs for the Strickland Trace.

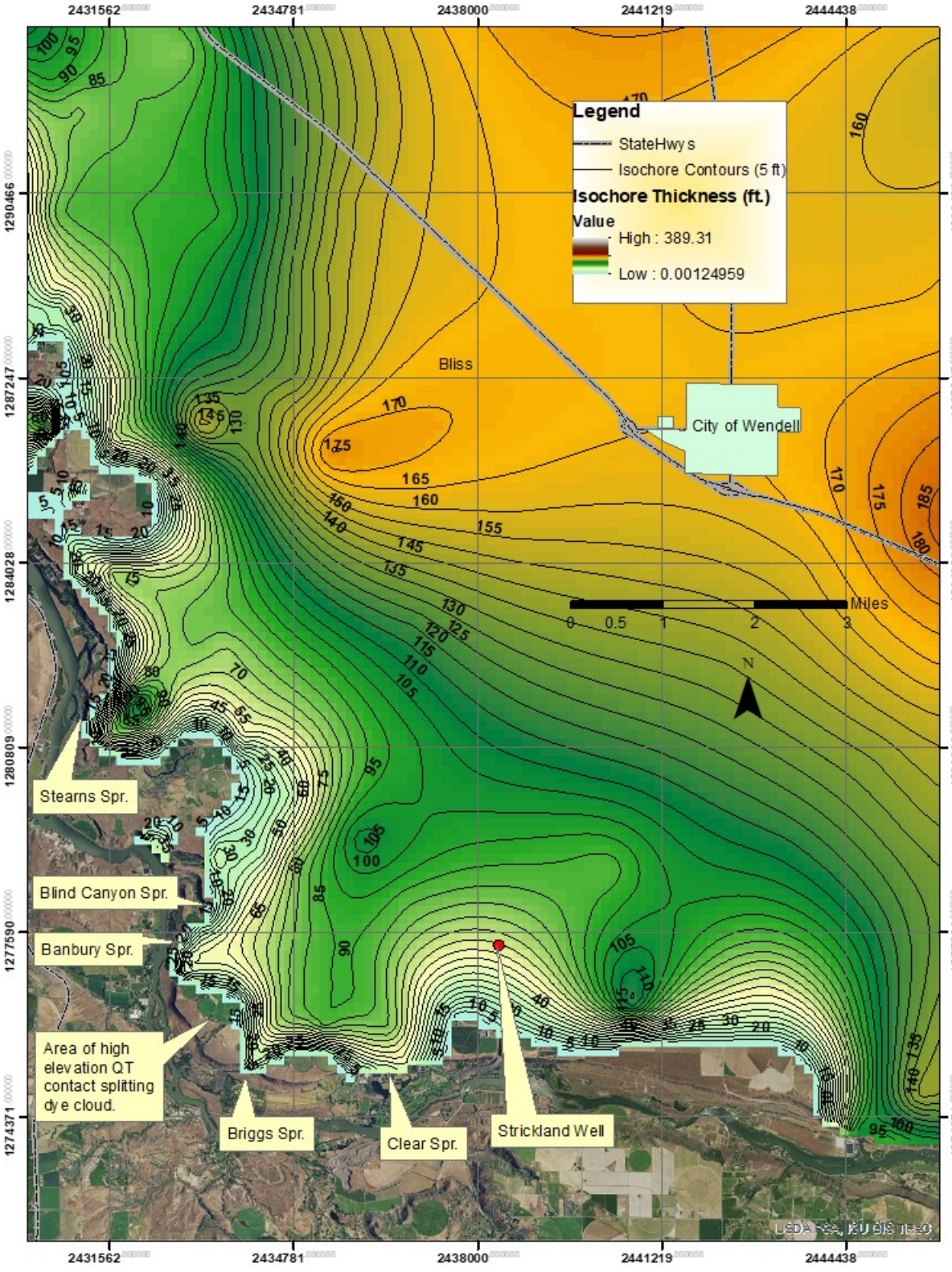

Figure 16. Isochore thicknes map of the aquifer in feet units and contour lines in 5 foot intervals. The isochore thicknes is a 'plumb' distance between the water table and the QT contact surfaces which results in an aquifer saturated thickness for the high 'K' zone within the Quaternary rocks. Perimeter graticules are IDTM meter units.

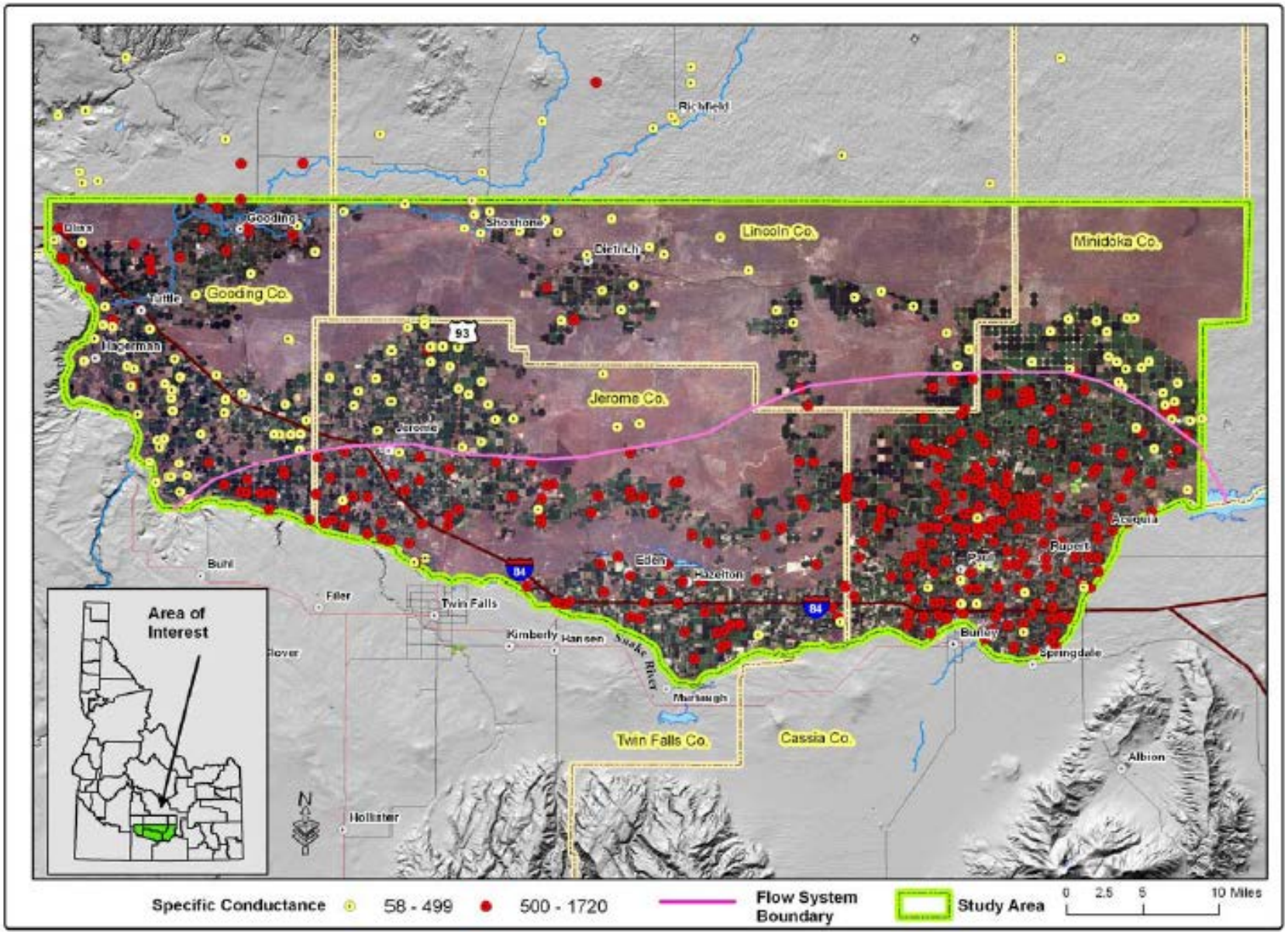

Figure 17. Flow system boundary based on specific conductivity. Adapted from Baldwin et al (2006)

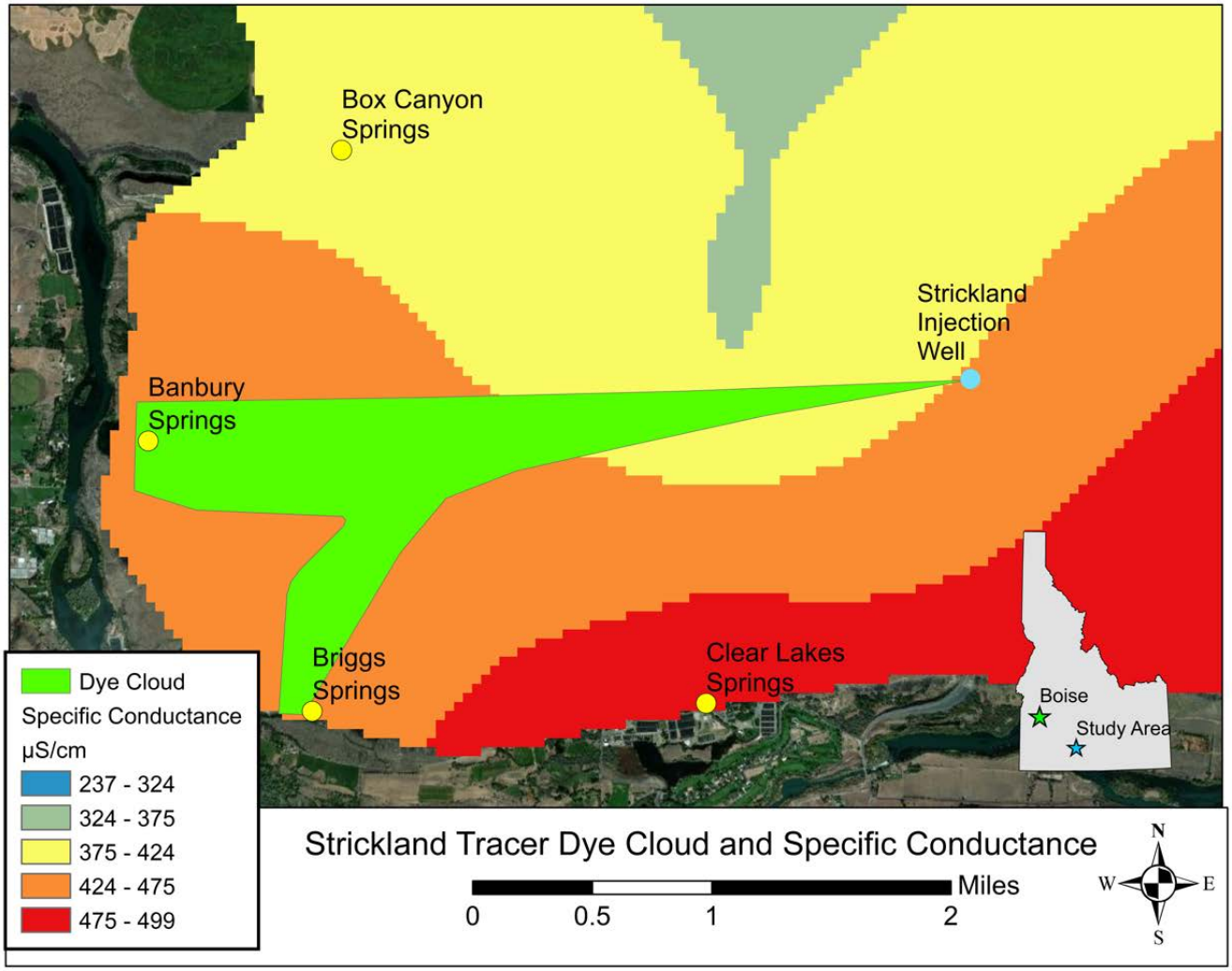

Figure 18. Isopleths of specific conductance from 2011 synoptic well measurements.

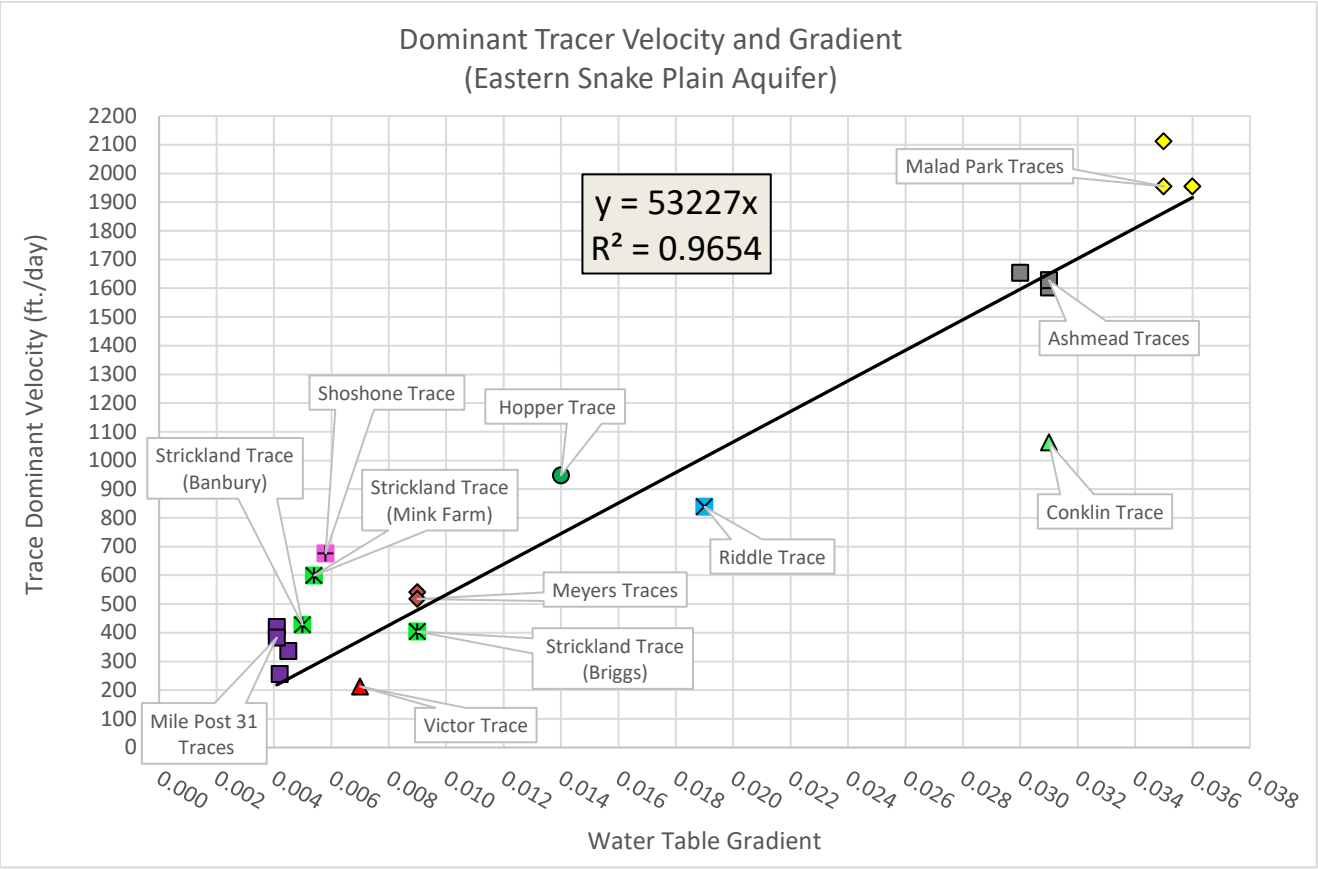

Figure 19. Relation between dominant tracer velocity and water table gradient for various tracers completed on the ESPA. This chart shows a high degree of proportionality which means our traces conform to Darcy's Law.

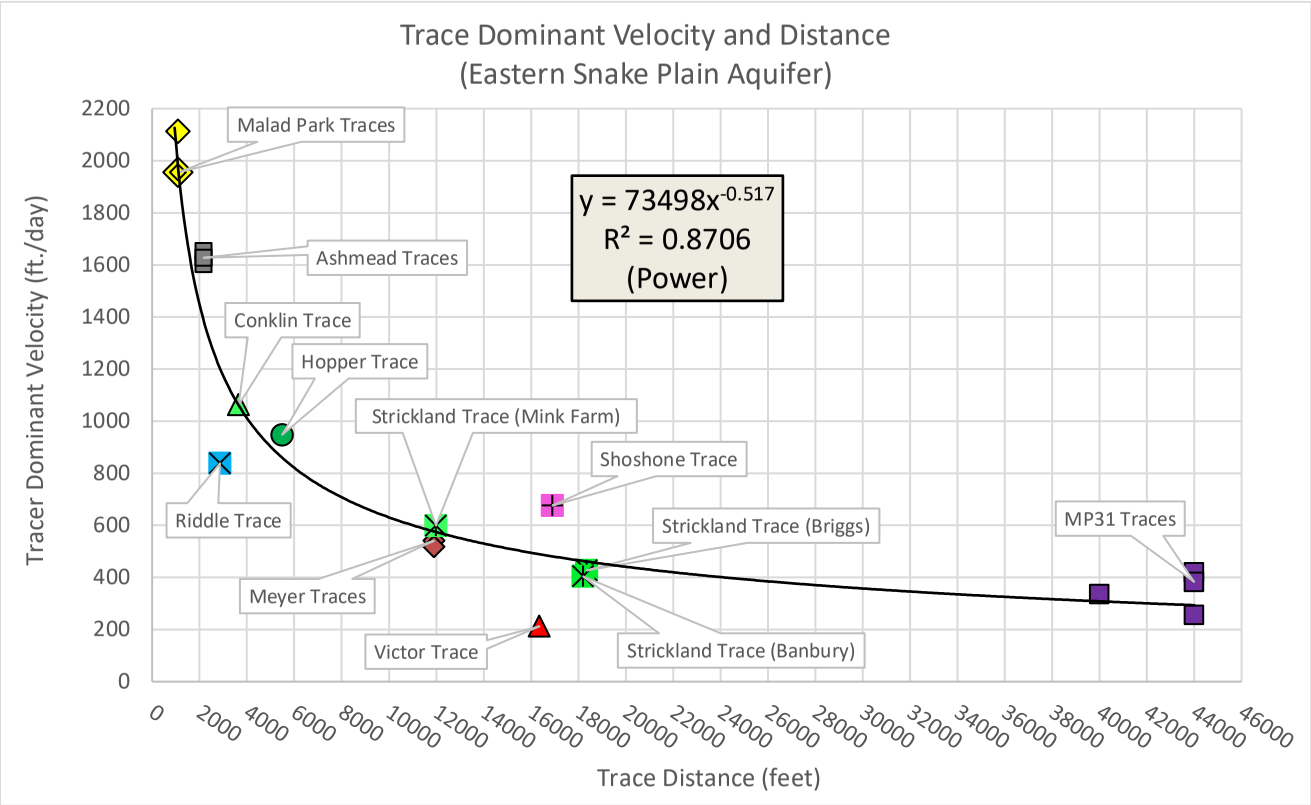

Figure 20. Relation between dominant tracer velocity and distance for various tracers completed on the ESPA.

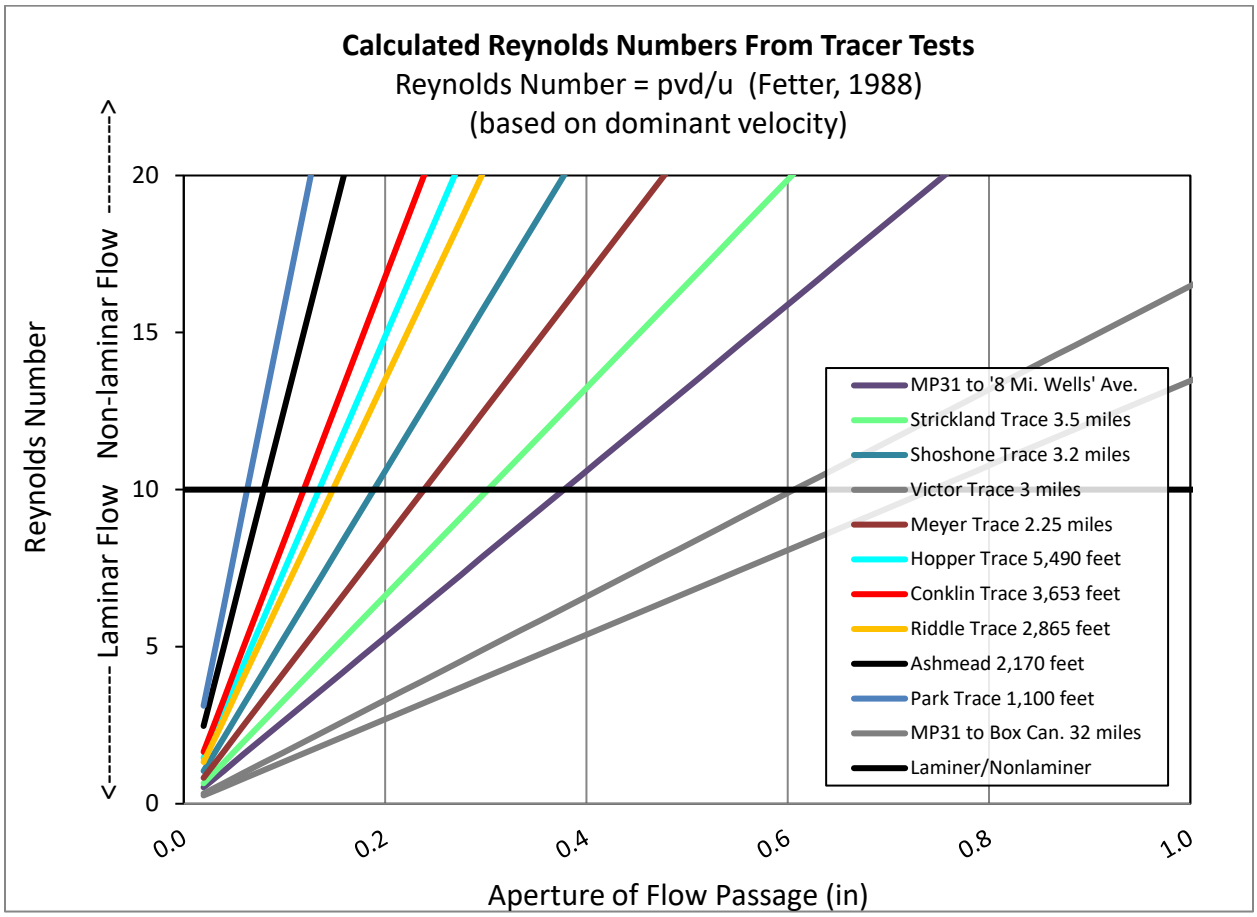

Figure 21. Calculated Reynolds Numbers (Re) for tracer studies on the lower basin ESPA. Re is calculated using dominant velocity and a continuum of flow passage apertures.

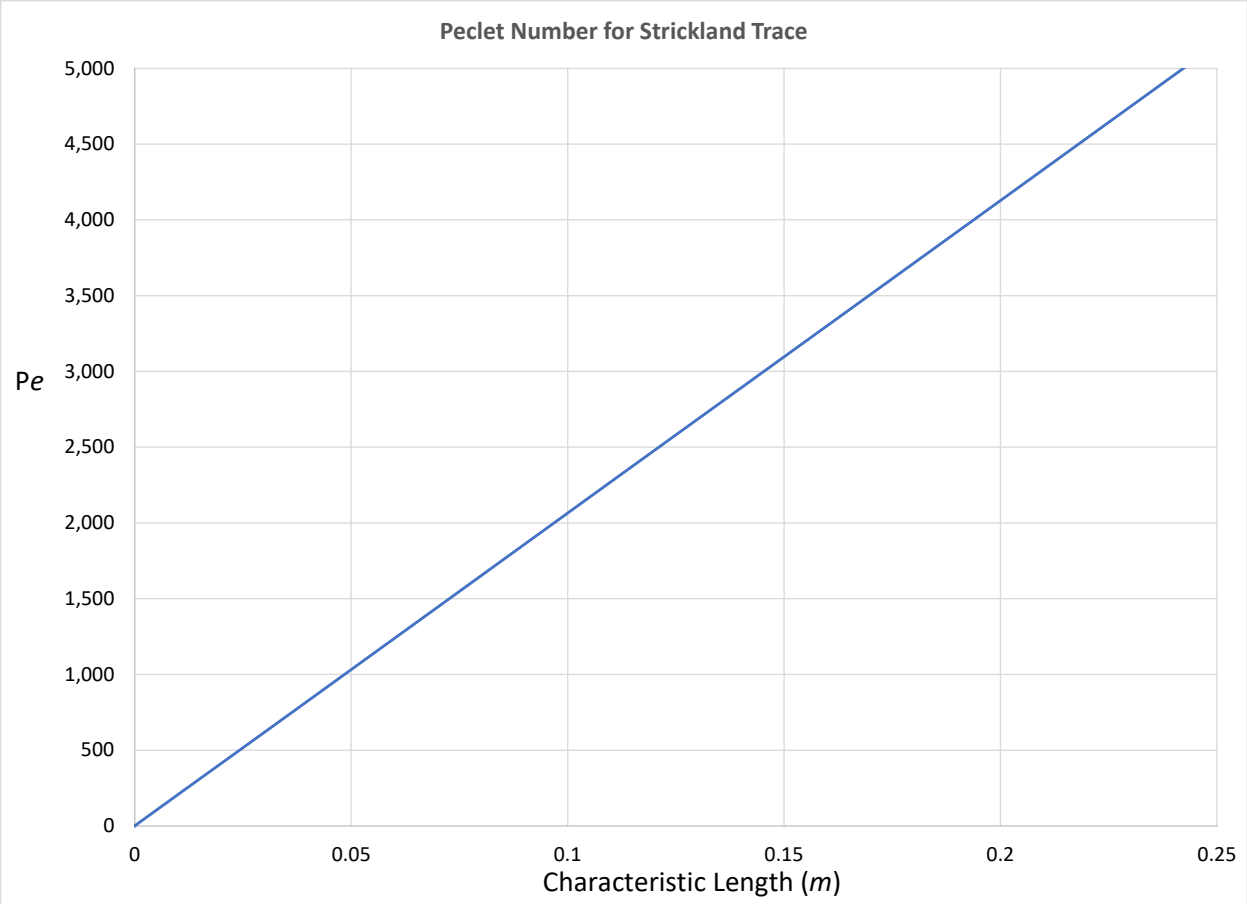

Figure 22. Peclet chart for the Strickland Trace.

REFRENCES SITED

Aley, T. (2002). *The Ozark Underground Laboratory's Ground Water Tracing Handbook.* Retrieved from www.ozarkundergroundlab.com

Aley, T., & Beeman, S. (2015). *Procedures and Criteria Analysis of Fluorescent Dyes in Water and Charcaol Samplers: Fluoresceind, Eosine, Rhodamine WT, and Sulforhodamine B Dyes*. Retrieved from Protem, MO:

Covington, H.R. and Weaver, J.N., 1990-1991, Geologic maps of the north wall of the Snake River canyon, Thousand Springs, and Niagara Springs Quadrangles, Idaho, U.S. Geological Survey Map Series I-1947-C.

Baldwin, J., Winter, G., & Dai, X. (2006). *2005 Update, Thousand Springs Area of the Eastern Snake River Plain, Idaho.* Idaho Department of Environmental Quality.

Farmer, N., & Blew, D. (2022). *Evidence from dye tracing for both preferential and non-preferential flow in a fractured Basalt aquifer, south Idaho.* National Ground Water Association Conference, Burlington, VT.

Farmer, N., & Blew, D. (2009). *Fluorescent Dye Tracer Tests at the Malad Gorge State Park.* Boise, ID: http://www.idwr.idaho.gov/files/publications/20100519-OFR-Malad-Gorge-Trace-at-Riddle-well.pdf Retrieved from http://www.idwr.idaho.gov/files/publications/20090930-OFR-Malad-Gorge-Tracer-Tests.pdf.

Farmer, N., & Blew, D. (2010). *Fluorescent Dye Tracer Test near the Malad Gorge State Park (Riddle Well Test).* Boise, ID: Idaho Department of Water Resources Retrieved from http://www.idwr.idaho.gov/files/publications/20100519-OFR-Malad-Gorge-Trace-at-Riddle-well.pdf.

Farmer, N., & Blew, D. (2011). *Fluorescent Dye Tracer Test and Hydrogeology Near the Malad Gorge State Park (Hopper Well Test)*. Boise, ID: Idaho Department of Water Resources Retrieved from http://www.idwr.idaho.gov/files/publications/20110201-OFR-Hydrogeology-and-1-Mile-Dye-Trace-South-of-Malad-Gorge.pdf.

Farmer, N., & Blew, D. (2012). *Fluorescent Dye Tracer Tests and Hydrogeology near the Malad Groge State Park (Meyer, Conklin and Riddle Wells)*. Boise, ID: Idaho Department of Water Resources Retrieved from http://www.idwr.idaho.gov/files/publications/201204-OFR-Hydrogeology-and-2-25-Mile-Dye-Trace-South-of-Malad-Gorge.pdf.

Farmer, N., & Blew, D. (2014a). *Fluorescnet Dye Tracer Tests Near Clear Lakes from the 'Ashmead' Well*. Boise, ID: Idaho Department of Water Resources Retrieved from http://www.idwr.idaho.gov/files/publications/20140218-OFR-Clear-Springs-Hydrogeology-and-Ashmead-Well-Dye-Trace.pdf.

Farmer, N., Blew, D., & Aley, T. (2014b). *Fluorescent Dye Tracer Tests from the Victor Well South East of the Malad Gorge State Park.* Boise, ID Idaho Department of Water Resources Retrieved from http://www.idwr.idaho.gov/files/publications/20141002-OFR-Victor-Well-Dye-Tracer-Test.pdf.

Farmer, N., & Blew, D. (2018). *Box Canyon Tracer*. Unpublished Data.

Fetter, C.W. (1988) Applied Hydrogeology. 2nd Edition, Merrill Publishing Company, London.

Garabedian, S.P., 1992, Hydrology and digital simulation of the regional aquifer system, eastern Snake River plain, Idaho, U.S. Geological Survey Professional Paper 1408-F.

Johnson, A.I., 1965, Determination of hydrologic and physical properties of volcanic rocks by laboratory methods, in Wadia, D.N., ed., Commemorative volume: Mining and Metallurgical Institute of India, p. 50-63 and 78.

Kingscote Chemicals, 2022, Water Tracing Dye Fluorescein, Technical Data Bulletin, www.kingscotechemicals.com

Lindholm, G.F., 1993, Summary of the Snake River plain regional aquifer-system analysis in Idaho and eastern Oregon, U.S. Geological Survey Open-File Report 91-98, 62 p.

Lindholm, G.G., 1996, Summary of the Snake River plain regional aquifer-system analysis in Idaho and eastern Oregon, U.S. Geological Survey Professional Paper 1408-A, A-59 p.

Low, W.H., 1987, Solute distribution in ground and surface water in the Snake River basin, Idaho and eastern Oregon: U.S. Geological Survey Hydrologic Investigations Atlas HA-696, scale 1:1,000,000, 2 sheets.

Ma, R., C. Zheng, J. M. Zachara, and M. Tonkin (2012), Utility of bromide and heat tracers for aquifer characterization affected by highly transient flow conditions, Water Resour. Res., 48, W08523, doi:10.1029/2011WR011281.

Malde, H.E., 1991, Quaternary geology and structural history of the Snake River Plain, Idaho and Oregon in Morrison, R.B., ed., Quaternary nonglacial geology; conterminous U.S.: Boulder, CO, Geological Society of America, The Geology of North America, vol. K-2.

Malde, H.E., 1982, The Yahoo Clay, a lacustrine unit impounded by the McKinney Basalt in the Snake River canyon near Bliss, Idaho, in Bonnichsen, B., and Breckenridge, R.M., eds., Cenozoic geology of Idaho: Idaho Bureau of Mines and Geology Bulletin 26, p. 617-628.

Malde, H.E., 1972, Stratigraphy of the Glenns Ferry Formation from Hammett to Hagerman, Idaho: U.S. Geological Survey Bulletin 1331-D, 19 p.

Malde, H.E., 1971, History of Snake River canyon indicated by revised stratigraphy of Snake River group near Hagerman and King Hill, Idaho, Shorter contributions to general

geology; Geological Survey professional paper, 644-F, 21 p.

Marking, L., Leif, 1969, Toxicity of Rhodamine b and Fluorescein sodium to fish and their compatibility with antimycin A, The Progressive Fish Culturist, vol. 31, July 1969, no. 3. 139-142 p.

Meinzer, O.E., 1927, Large springs in the United States, USGS Water Supply Paper 557, library number (200) G no.557, 94 p.

Whitehead, R.L., 1992, Geohydrologic framework of the Snake River plain regional aquifer system, Idaho and eastern Oregon, U.S. Geological Survey Professional Paper 1408-B.

Whitehead, R.L., 1992, Generalized geologic profiles of the north wall of the Snake River canyon from King Hill to Milner, Snake River plain, Idaho and eastern Oregon, U.S. Geological Survey Professional Paper 1408-B, Plate #2.

Whitehead, R.L., and Lindholm, G.F., 1985, Results of geohydrologic test drilling in the eastern Snake River plain, Gooding county, Idaho, U.S. Geological Survey, Water Resources Investigation Report 84-4294, 30 p.

Worthington, Stephen & Soley, Robert. (2017). Identifying turbulent flow in carbonate aquifers. Journal of Hydrology. 552. 10.1016/j.jhydrol.2017.06.045.

OTHER REFERENCES AND SOURCES OF INFORMATION

1. Anderson, M.P., 2005, Heat as a ground water tracer, Ground Water Journal, November-December, Vol. 43, No. 6, pages 951-968.

2. Anderson, M. P. and Woessner, W. W., 1992, Applied groundwater modeling, Academic Press, San Diego.

3. Anderson, M.P., 1979, Using models to simulate the movement of contaminants through groundwater flow systems, Critical Reviews in Environmental Controls 9, no. 2: 97-156.

4. Aulenbach, D.B., Bull, J.H., and Middlesworth, B.C., 1978, Use of tracers to confirm ground-water flow: Ground Water, Vol. 16, No. 3, 149-157 p.

5. Axelsson, G., Bjornsson, G., and Montalvo, F., 2005, Quantitative interpretation of tracer test data, Proceedings World Geothermal Congress, 24-29 p.

6. Baldwin, J., Brandt, D., Hagan, E., and Wicherski, B., 2000, Cumulative impacts assessment, Thousand Springs area of the eastern snake river plain Idaho, Department of Environmental Quality, Ground Water Quality Technical Report No. 14, 56 p.

7. Baldwin, J., Winter, G., and Dai, Xin, 2005 update, thousand springs area of eastern snake plain Idaho, Department of Water Quality, Ground Water Quality Technical Report No. 27, 2006, 73 p.

8. Blew, D., and Scheidt, N., 2006, verbal communication for unpublished data from field flow measurement exercise to determine leakage from the Little Wood river.

9. Bonnichsen, B., and Godchaux, M.M., 2002, Late Miocene, Pliocene, and Pleistocene Geology of Southwestern Idaho With Emphasis on Basalts in the Bruneau-Jarbidge, Twin Falls, and Western Snake River Plain Regions; Tectonic and Magmatic Evolution of the Snake River Plain Volcanic Province, Idaho Geological Survey, Bulletin 30, 482 p.

10. Bonnichsen, B., McCurry, M., and White, C.M., 2002, Tectonic and Magmatic Evolution of the Snake River Plain Volcanic Province, Idaho Geological Survey Bulletin 30, 482 p.

11. Bowler, P.A., Watson, C.M., Yearsley, J.R., Cirone, P.A., 1992, Assessment of ecosystem quality and its impact on resource allocation in the middle Snake River sub- basin; (CMW, JRY, PAC - U.S. Environmental Protection Agency, Region 10; PAB - Department of Ecology and Evolutionary Biology, University of California, Irvine), Desert Fishes Council (http://www.desertfishes.org/proceed/1992/24abs55.html).

12. Chen-Northern, Inc., 1991, Hydrogeologic assessment at Clear Lakes grade, Gooding county, Idaho, Idaho State Department of Transportation, Key # 03586 and Key # 05849, Boise Idaho State Street office, prepared by Paul Spillers, 44 p. plus appendices. (hard copy on file at IDWR).

13. Covington, H.R., and Weaver, J. N., 1991, Geologic maps and profiles of the north wall of the Snake river canyon, Thousand springs and Niagra springs quadrangles, Idaho, U.S. Geological Survey, Miscellaneous Investigation Series, Map I-1947-C.

14. Covington, H.R., Whitehead, R.L., and Weaver, J.N., 1985**,** Ancestral canyons of the Snake River; geology and geohydrology of canyon-fill deposits in the Thousand Springs area, south-central Snake River Plain, Idaho: Geological Society of America Rocky Mountain Section, 38th Annual Meeting, Boise, Idaho, 1985, Composite Field Guide, Trip 7, 30 p.

15. Crandall, L., 1918, The springs of the Snake River canyon, Idaho Irrigation, Engineering, and Agriculture Societies Joint Conference Proceeding, pp. 146-150.

16. Dallas, K., 2005, Hydrologic study of the Deer Gulch basalt in Hagerman fossil beds national monument, Idaho, thesis, 96 p.

17. Davies, G.J., 2000, Lemon lane landfill investigation, Technical Note: Groundwater tracing using fluorescent dyes: interpretation of results and its implications, The Coalition Opposed to PCB Ash in Monroe County, Indiana, 24 p.

18. Davis, S., Campbell, D.J., Bentley, H.W., Flynn T.J., 1985, Ground water tracers, 200 p.

19. Dole, R.B., 1906, Use of Fluorescein in the study of underground waters, pg 73, USGS Water Supply Paper, #160, series 0, Underground Waters, 58, by Fuller M.L., 104 p.

20. Domenico P.A. and Schwartz F.W., 1990, Physical and chemical hydrogeology, John wiley & sons, 824 p.

21. Farmer, N. 2021, Idaho Water Resources Research Institute Seminar Series, Sept. 21st.

22. Farmer, N., and Blew, D., 2016, Unpublished data from dye trace at Mile Post 31 aquifer recharge site.

23. Farmer, N., Blew, D., Aley, T., 2014, Fluorescent dye tracer tests from the Victor well south east of the Malad gorge state park, Idaho Department of Water Resources Open File Report, 55 p. + Table of Results.

24. Farmer, N., and Blew, D., 2014, Fluorescent dye tracer tests near Clear Lakes from the Ashmead well, Idaho Department of Water Resources Open File Report, 50 p. + Table of Results.

25. Farmer, N., and Blew, D., 2013, Unpublished data from dye trace at Strickland well.

26. Farmer, N., and Blew, D., 2011, Fluorescent dye tracer tests and hydrogeology near the Malad Gorge state park (Hopper well test), Idaho Department of Water Resources Open File Report, 41 p.

27. Farmer, N., and Blew, D., 2010, Fluorescent dye tracer tests near the Malad Gorge state park (Riddle well test), Idaho Department of Water Resources Open File Report, 36 p.

28. Farmer, N., 2009, Review of hydrogeologic conditions located at and near the spring at Rangen inc., Idaho Department of Water Resources open file report, 46 p.

29. Farmer, N., and Owsley, D., 2009, Fluorescent dye tracer test at the W-canal aquifer recharge site, Idaho Department of Water Resources Open File Report, 23 p.

30. Farmer, N., and Blew D., 2009, Fluorescent dye tracer tests at Malad Gorge state park, Idaho Department of Water Resources Open File Report, 45 p.

31. Farmer, N., 2008, Traffic jams occur in nature too – geologic architecture of Hagerman valley spring discharge areas, Idaho Water Resource Research Institute Ground Water Connections Conference, Sept. 23 & 24, Boise, Idaho, Session 4 Research.

32. Farmer, C.N., and Nagai, O., 2004, Non-native vegetation growth patterns as a tracer for development of human caused perched aquifers in landslide areas, Journal of the Japan Landslide Society, vol. 41, no. 3 (161), 12 p.

33. Farmer N., and Larsen, I., 2001, Ground water tracer tests at the Hagerman fossil beds national monument, unpublished U.S. Dept. of Interior, National Park Service technical report, January 2001, 21 p.

34. Farmer N., 1998, Hydrostratigraphic model for the perched aquifer systems located near Hagerman fossil beds national monument, Idaho, University of Idaho thesis, 106 p.

35. Fetter, C.W., 1988, Applied hydrogeology, second edition, Macmillan publishing company, 592 p.

36. Fetter, C.W., 1993, Contaminant hydrogeology, Macmillan publishing company, 458 p.

37. Field, M.S., Wilhelm R.G., Quinlan J.F. and Aley T.J., 1995, An assessment of the potential adverse properties of fluorescent tracer dyes used for groundwater tracing, Environmental Monitoring and Assessment, vol. 38, 75-96 p.

38. Gaikowski, M.P., Larson, W.J., Steuer, J.J., Gingerich, W.H., 2003, Validation of two dilution models to predict chloramine-T concentrations in aquaculture facility effluent, Aquacultural Engineering 30, 2004, 127-140 p.

39. Galloway, J.M., 2004, Hydrogeologic characteristics of four public drinking water supply springs in northern Arkansas, U.S. Geological Survey Water-Resources Investigations Report 03-4307, 68 p.

40. Harvey, K.C., 2005, Beartrack mine mixing zone dye tracer study outfall 001, Napias creek Lemhi county, Idaho, Private Consulting Report by KC Harvey, LLC., 59 p.

41. Hudson, B.G. and Moran, J.E., 2002, Delineation of fast flow paths in porous media using noble gas tracers, U.S. Dept. of Energy Lawrence Livermore National Laboratory, CA., 18 p.

42. Idaho Department of Water Resources, 2018, ESPA groundwater contours.

43. Kauffman, J. D., Othberg, J. S., Shervais, J., Cooke, M., 2005, Geologic Map of the Shoshone Quadrangle, Lincoln, County, Idaho: Idaho Geological Survey digital web DWM-44.

44. Kass, W. et. al., 2009, Tracing technique in geohydrology, reprinted by CRC Press from year 1998 publishers A.A. Balkema, 581 p.

45. Kilpatrick, F.A. and Cobb, E.D., 1985, Measurement of discharge using tracers, U.S. Geological Survey Techniques of Water-Resources Investigations Report, book 3, chapter A16.

46. Klotz, D., Seiler K.P., Moser H., and Neumaier F., 1980, Dispersivity and velocity relationship from laboratory and field relationships. Journal of Hydrology 45, no. 3: 169-84.

47. Leet, D., Judson, S. and Kauffman, M., 1978, Physical Geology, 5th edition, ISBN 0-13-669739-9, 490 p.

48. Leibundgut, C. and H. R. Wernli. 1986. Naphthionate--another fluorescent dye. Proc. 5th Intern'l. Symp. on Water Tracing. Inst. of Geol. & Mineral Exploration, Athens, 167-176 p.

49. Malde, H.E., 1991, Quaternary geology and structural history of the Snake River Plain, Idaho and Oregon in Morrison, R.B., ed., Quaternary nonglacial geology; conterminous U.S.: Boulder, CO, Geological Society of America, The Geology of North America, vol. K-2.

50. Malde, H.E., 1982, The Yahoo Clay, a lacustrine unit impounded by the McKinney Basalt in the Snake River canyon near Bliss, Idaho, in Bonnichsen, B., and Breckenridge, R.M., eds., Cenozoic geology of Idaho: Idaho Bureau of Mines and Geology Bulletin 26, p. 617-628.

51. Malde, H.E., 1972, Stratigraphy of the Glenns Ferry Formation from Hammett to Hagerman, Idaho: U.S. Geological Survey Bulletin 1331-D, 19 p.

52. Malde, H.E., 1971, History of Snake River canyon indicated by revised stratigraphy of Snake River group near Hagerman and King Hill, Idaho, Shorter contributions to general geology; Geological Survey professional paper, 644-F, 21 p.

53. Marking, L., Leif, 1969, Toxicity of Rhodamine b and Fluorescein sodium to fish and their compatibility with antimycin A, The Progressive Fish Culturist, vol. 31, July 1969, no. 3. 139-142 p.

54. Meinzer, O.E., 1927, Large springs in the United States, USGS Water Supply Paper 557, library number (200) G no.557, 94 p.

55. Moser, H., 1995, Groundwater tracing, Tracer Technologies for Hydrological Systems (Proceedings of a Boulder Symposium, July 1995), IAHS Publ. No. 229, 1995.

56. Mull, D.S., Liebermann, T.D., Smoot, J.L., Woosley, L.H. Jr., (U.S. Geological Survey), 1988, Application of dye-tracing techniques for determining solute-transport characteristics of ground water in karst terrranes; U.S. EPA904/6-88-001, 103 p.

57. Noga, E.J., and Udomkusonsri, P., 2002, Fluorescein: a rapid, sensitive, non-lethal method for detecting skin ulceration in fish, Vet Pathol 39:726–731 p.

58. Othberg, K.L. and Kauffman, J.D., 2005, Geologic map of the Bliss quadrangle, Gooding, and Twin Falls counties, Idaho, Idaho Geological Survey map #53.

59. Otz, M. H., and Azzolina, N.A., 2007, Preferential ground-water flow: evidence from decades of fluorescent dye-tracing, Geological Society of America fall meetings presentation, 19 slides.

60. Olsen, L.D. and Tenbus F.J., 2005, Design and analysis of a natural-gradient groundwater tracer test in a freshwater tidal wetland, west branch canal creek, Aberdeen proving ground, Maryland, U.S. Geological Survey Scientific Investigation Report 2004-5190, 116 p.

61. Parker, G.G., 1973, Tests of Rhodamine WT dye for toxicity to oysters and fish, Journal of Research U.S. Geological Survey, Vol. 1, No. 4, July-Aug., 499 p.

62. Quinlan, J.F. and Koglin, E.N. (EPA), 1989, Ground-water monitoring in karst terrranes: recommended protocols and implicit assumptions, U.S. Environmental Protection Agency, EPA 600/x-89/050, IAG No. DW 14932604-01-0, 79 p.

63. Quinlan, J.F., 1990, Special problems of ground-water monitoring in karst terranes, Ground Water and vadose Zone Monitoring, ASTM STP 1053, D.M. Nielsen and A.I. Johnson, (Eds), American Society for Testing and Materials, Philadelphia, p. 275 -304.

64. Ralston, D., 2008, Hydrogeology of the thousand springs to Malad reach of the enhanced snake plain aquifer model, Idaho Department of Water Resources report, 20 p.

65. Russell, I.C., 1902, Geology and water resources of the Snake river plains of Idaho, USGS Bulletin 199, library number (200) E no.199, 192 p.

66. Schmidt, R., and Salovich, M., 1998, Analytic element flow modeling the mile post 31 recharge site., Guidance for Developing a Ground Water Quality Monitoring Program for Managed Recharge Projects by Land Application, June 2010, Idaho Department of Environmental Quality.

67. Schorzman, K., Baldwin, J., and Bokor, J., 2009, Possible sources of nitrate to the springs of southern Gooding county, eastern snake river plain, Idaho, Department of Environmental Quality, Ground Water Quality Technical Report No. 38, 41 p.

68. Shervais, J., Evans, J.P., Lachmar, T.E., Christiansen, E.J., Schmitt, D.R., Kessler, J.E., Potter, K. E., Jean, M.M., Sant, C.J., Freeman, T.G., Project hotspot – the Snake river scientific drilling project: a progress report, Geological Society of America Rocky Mountain 63rd Annual meeting and Cordilleran 107th Annual meeting May 18-20, 2011, Abstracts with Programs, Vol. 43, No. 4, p. 5.

69. Smart, C. and Simpson B.E., 2002, Detection of fluorescent compounds in the environment using granular activated charcoal detectors, Environmental Geology, vol. 42, 538-545 p.

70. Smart, P.L., 1984, A review of the toxicity of twelve fluorescent dyes used for water tracing, National Speleological Society publication, vol. 46, no. 2: 21-33.

71. Smart, P.L., 1984, A review of the toxicity of twelve fluorescent dyes used for water tracing, National Speleological Society publication, vol. 46, no. 2: 21-33.

72. Spangler, L.E., and Susong, D.D., 2006, Use of dye tracing to determine ground-water movement to Mammoth Crystal springs, Sylvan pass area, Yellowstone national park, Wyoming, U.S. Geological Survey Scientific Investigations Report 2006-5126, 19 p.

73. Stearns, H.T., 1983, Memoirs of a geologist: from Poverty peak to Piggery gulch, Hawaii Institute of Geophysics, 242 p.

74. Stearns, H.T., Crandall, L., Steward, W.G., 1938, Geology and ground-water resources of the Snake River plain in southeastern Idaho; U.S. Geological Survey Water Supply Paper 774, 268 p.

75. Stearns, H. T., 1936, Origin of large springs and their alcoves along the snake river in southern Idaho, The Journal of Geology, vol. 44, No. 4, 429-450 p.

76. Taylor, C.J., and Greene E.A., Hydrogeologic characterization and methods used in the investigation of karst hydrology, U.S. Geological Survey field techniques for estimating water fluxes between surface water and ground water, chapter 3, Techniques and Methods 4-D2, 71-114 p.

77. Taylor, C.J., and Alley, W.M., 2001, Ground-water-level monitoring and the importance of long-term water-level data, U.S. Geological Survey Circular 1217, 68 p.

78. U.S. Army Corps of Engineers, 1983, Interim Feasibility Report – Clear Lakes Hydropower Snake River, Idaho, Upper Snake River and Tributaries, for Idaho Water Resource Board, 62 p. (original hard copy on file at IDWR)

79. Walthall, W.K., and Stark J.D., 1999, The acute and chronic toxicity of two xanthene dyes, Fluorescein sodium salt and phloxine B, to Daphnia pulex, Environmental Pollution volume 104, 207-215 p.

80. Wilson, J.F., Cobb, E.D., and Kilpatrick F.A., 1986, Fluorometric procedures for dye tracing, U.S. Geological Survey Techniques of Water-Resources Investigations of the United States Geological Survey, Applications of Hydraulics, book 3, chapter A12, 43 p.

81. Unpublished data, 2016, Blew, D., Farmer, N., Dye tracer tests at Mile Post 31 and Strickland locations.